

# SIXTH ORDER COMPACT FINITE DIFFERENCE METHOD FOR 2D HELMHOLTZ EQUATIONS WITH SINGULAR SOURCES AND REDUCED POLLUTION EFFECT

QIWEI FENG, BIN HAN, AND MICHELLE MICHELLE

ABSTRACT. Due to its highly oscillating solution, the Helmholtz equation is numerically challenging to solve. To obtain a reasonable solution, a mesh size that is much smaller than the reciprocal of the wavenumber is typically required (known as the pollution effect). High order schemes are desirable, because they are better in mitigating the pollution effect. In this paper, we present a sixth order compact finite difference method for 2D Helmholtz equations with singular sources, which can also handle any possible combinations of boundary conditions (Dirichlet, Neumann, and impedance) on a rectangular domain. To reduce the pollution effect, we propose a new pollution minimization strategy that is based on the average truncation error of plane waves. Our numerical experiments demonstrate the superiority of our proposed finite difference scheme with reduced pollution effect to several state-of-the-art finite difference schemes in the literature, particularly in the critical pre-asymptotic region where  $kh$  is near 1 with  $k$  being the wavenumber and  $h$  the mesh size.

## 1. INTRODUCTION AND MOTIVATIONS

In this paper, we study the 2D Helmholtz equation, which is a time-harmonic wave propagation model, with a singular source term along a smooth interface curve and mixed boundary conditions. Let  $\Omega = (l_1, l_2) \times (l_3, l_4)$  and  $\psi$  be a smooth two-dimensional function. Consider a smooth curve  $\Gamma_I := \{(x, y) \in \Omega : \psi(x, y) = 0\}$ , which partitions  $\Omega$  into two subregions:  $\Omega^+ := \{(x, y) \in \Omega : \psi(x, y) > 0\}$  and  $\Omega^- := \{(x, y) \in \Omega : \psi(x, y) < 0\}$ . The model problem is explicitly defined as follows:

$$\begin{cases} \Delta u + k^2 u = f & \text{in } \Omega \setminus \Gamma_I, \\ [u] = g_D, \quad [\nabla u \cdot \vec{n}] = g_N & \text{on } \Gamma_I, \\ \mathcal{B}_1 u = g_1 \text{ on } \Gamma_1 := \{l_1\} \times (l_3, l_4), \quad \mathcal{B}_2 u = g_2 \text{ on } \Gamma_2 := \{l_2\} \times (l_3, l_4), \\ \mathcal{B}_3 u = g_3 \text{ on } \Gamma_3 := (l_1, l_2) \times \{l_3\}, \quad \mathcal{B}_4 u = g_4 \text{ on } \Gamma_4 := (l_1, l_2) \times \{l_4\}, \end{cases} \quad (1.1)$$

where  $k$  is the wavenumber,  $f$  is the source term, and for any point  $(x_0, y_0) \in \Gamma_I$ ,

$$[u](x_0, y_0) := \lim_{(x,y) \in \Omega^+, (x,y) \rightarrow (x_0, y_0)} u(x, y) - \lim_{(x,y) \in \Omega^-, (x,y) \rightarrow (x_0, y_0)} u(x, y), \quad (1.2)$$

$$[\nabla u \cdot \vec{n}](x_0, y_0) := \lim_{(x,y) \in \Omega^+, (x,y) \rightarrow (x_0, y_0)} \nabla u(x, y) \cdot \vec{n} - \lim_{(x,y) \in \Omega^-, (x,y) \rightarrow (x_0, y_0)} \nabla u(x, y) \cdot \vec{n}, \quad (1.3)$$

where  $\vec{n}$  is the unit normal vector of  $\Gamma_I$  pointing towards  $\Omega^+$ . In (1.1), the boundary operators  $\mathcal{B}_1, \dots, \mathcal{B}_4 \in \{\mathbf{I}_d, \frac{\partial}{\partial \vec{n}}, \frac{\partial}{\partial \vec{n}} - ik\mathbf{I}_d\}$ , where  $\mathbf{I}_d$  corresponds to the Dirichlet boundary condition (sound soft boundary condition for the identical zero boundary datum),  $\frac{\partial}{\partial \vec{n}}$  corresponds to the Neumann boundary condition (sound hard boundary condition for the identical zero boundary datum), and  $\frac{\partial}{\partial \vec{n}} - ik\mathbf{I}_d$  (with  $i$  being the imaginary unit) corresponds to the impedance boundary condition. Moreover, the Helmholtz equation of (1.1) with  $g_D = 0$  is equivalent to finding the weak solution  $u \in H^1(\Omega)$  of  $\Delta u + k^2 u = f + g_N \delta_{\Gamma_I}$  in  $\Omega$ , where  $\delta_{\Gamma_I}$  is the Dirac distribution along the interface curve  $\Gamma_I$ .

The Helmholtz equation is challenging to solve numerically due to several reasons. The first is due to its highly oscillatory solution, which necessitates the use of a very small mesh size  $h$  in many

---

2010 *Mathematics Subject Classification.* 65N06, 35J05.

*Key words and phrases.* Helmholtz equation, finite difference, pollution effect, interface, pollution minimization, mixed boundary conditions, corner treatment.

Research supported in part by Natural Sciences and Engineering Research Council (NSERC) of Canada under Grant RGPIN-2019-04276, and Alberta Innovates and Alberta Advanced Education.

discretization methods. Taking a mesh size  $h$  proportional to the reciprocal of the wavenumber  $k$  is not enough to guarantee that a reasonable solution is obtained or a convergent behavior is observed. The mesh size  $h$  employed in a standard discretization method often has to be much smaller than the reciprocal of the wavenumber  $k$ . In the literature, this phenomenon is referred to as the pollution effect, which has close ties to the numerical dispersion (or a phase lag). The situation is further exacerbated by the fact that the discretization of the Helmholtz equation typically yields an ill-conditioned coefficient matrix. Taken together, one typically faces an enormous ill-conditioned linear system when dealing with the Helmholtz equation, where standard iterative schemes fail to work [13].

To gain a better insight on how the mesh size requirement is related to the wavenumber, we recall some relevant findings on the finite element method (FEM) and finite difference method (FDM). Two common ways to quantify the pollution effect are through the error analysis and the dispersion analysis. In the FEM literature, the former route is typically used and the analysis is applicable even for unstructured meshes. The authors in [27] considered the interior impedance problem and discovered that the quasi-optimality in the  $hp$ -FEM setting can be achieved by choosing a polynomial degree  $p$  and a mesh size  $h$  such that  $p \geq C \log(k)$  (for some positive  $C$  independent of  $k, h, p$ ) and  $kh/p$  is small enough. The authors in [11] found that for sufficiently small  $k^{2p+1}h^{2p}$ , the leading pollution term in an upper bound of the standard Sobolev  $H^1$ -norm is  $k^{2p+1}h^{2p}$ . This coincides with the numerical dispersion studied in [1, 24]. Meanwhile, the pollution effect in the FDM setting is studied via the dispersion analysis. That is, we analyze the difference between the true and numerical wavenumbers. For order 2 FDMs, [6, 7] found that  $k^3h^2 \leq C$  (for some positive  $C$  independent of  $k, h$ ) is required to obtain a reasonable solution. Meanwhile, for order 4 FDM, [9] found that  $k^5h^4 \leq C$  (for some positive  $C$  independent of  $k, h$ ) is required to obtain a reasonable solution. From the previous discussion, it is clear that the grid size requirement for high order schemes is less stringent than low order ones. This is why we focus on the construction of a high order scheme in the present paper.

A lot of research effort has been invested in developing ways to cope with the enormous ill-conditioned linear system arising from a discretization of the Helmholtz equation. Various preconditioners and domain decomposition methods have been developed over the years (see the review paper [18] and references therein). Many variants of FEM/Galerkin/variational methods have been explored. For example, [16, 17] relaxed the inter-element continuity condition and imposed penalty terms on jumps across the element edges. These penalty terms can be tuned to reduce the pollution effect. A class of Trefftz methods, where the trial and test functions consist of local solutions to the underlying (homogeneous) Helmholtz equation, were considered in [23] and references therein. The inter-element continuity in this kind of methods typically cannot be strongly imposed. Unfortunately, the pollution effect still persists in the  $h$ -refinement setting of these Trefftz methods. A closely related method, called the generalized FEM or the partition of unity FEM, has been explored. It involves multiplying solutions to the homogeneous Helmholtz equation (e.g. plane waves) with elements of a chosen partition of unity, which then serve as the trial and test functions. In recent years, multi-scale FEM has also become an appealing alternative to deal with the pollution effect [30]. From the perspective of FDM, one common approach is to use a scheme (preferably of high order) with minimum dispersion. We start with a stencil having a given accuracy order with some free parameters. Afterwards, we plug in the plane wave solution into the scheme and minimize the ratio between the true and numerical wavenumbers by forming an overdetermined linear system with respect to a set of discretized angles and a range of  $\frac{2\pi}{kh}$  (i.e., the number of points per wavelength). Such a procedure has been used in [6, 7, 9, 31, 35]. The resulting stencils have accuracy orders 2 in [6, 7], 4 in [9], and 6 in [35]. The number of points used in the proposed stencil varies from 9 in [6, 35], 13 in [10], and both 17 and 25 in [9]. Other studies on FDMs that do not explicitly consider the numerical dispersion are [3] (a 4th order compact FDM on polar coordinates), [4] (a 4th order compact FDM), [32] (a 6th order compact FDM), and [36] (a 6th order FDM with non-compact stencils for corners and boundaries). The authors in [29] proposed a 3rd order compact immersed interface method for our model problem. A characterization of the pollution effect in terms of eigenvalues was done in [12]. The authors in [8] showed that the order of the numerical dispersion matches the order of the finite

difference scheme for all plane wave solutions. Furthermore, by using an asymptotic analysis and modifying the wavenumber, they derived an FDM stencil for vanishing source terms whose accuracy for all plane wave solutions is of order 6. It is widely accepted that the pollution effect in standard discretizations arising from FEMs and FDMs cannot be eliminated for 2D and higher dimensions [2]. However, in 1D, we can obtain pollution free FDMs [20, 33], which are used to solve special 2D Helmholtz equations [20, 34].

There are only a few papers that deal with high order finite difference discretizations of mixed boundary conditions. The authors [4, 25, 32, 35] considered a square domain with Dirichlet and Robin boundary conditions. Furthermore, a method to handle flux type boundary conditions was discussed in [25]. The method of difference potentials was studied in [5, 26] to handle a domain with a smooth nonconforming boundary and mixed boundary conditions.

From the theoretical standpoint, as long as an impedance boundary condition appears on one of the boundary sides, the solution to (1.1) exists and is unique as studied in [19]. When an impedance boundary condition is absent, we shall avoid wavenumbers that lead to nonuniqueness. The rigorous stability analysis of the problem in (1.1) with  $g_D = g_N = 0$  was also done in [21, 22]. For the situation where  $g_D, g_N \neq 0$ , the well-posedness, regularity, and stability were rigorously studied in [28].

The main contributions of this paper are as follows. We derive a sixth order compact finite difference scheme with reduced pollution effect to solve (1.1)-(1.3) given the following assumptions:

- (A1) The solution  $u$  and the source term  $f$  have uniformly continuous partial derivatives of (total) orders up to seven and six respectively in each of the subregions  $\Omega^+$  and  $\Omega^-$ . However, both  $u$  and  $f$  may be discontinuous across the interface  $\Gamma_I$ .
- (A2) The interface curve  $\Gamma_I$  is smooth in the sense that for each  $(x^*, y^*) \in \Gamma_I$ , there exists a local parametric equation:  $\gamma : (-\epsilon, \epsilon) \rightarrow \Gamma_I$  with  $\epsilon > 0$  such that  $\gamma(0) = (x^*, y^*)$  and  $\|\gamma'(0)\|_2 \neq 0$ .
- (A3) The one-dimensional functions  $g_D \circ \gamma$  and  $g_N \circ \gamma$  have uniformly continuous derivatives of (total) orders up to eight and seven respectively on the interface  $\Gamma_I$ , where  $\gamma$  is given in (A2).
- (A4) Each of the functions  $g_1, \dots, g_4$  has uniformly continuous derivatives of (total) order up to seven on the boundary  $\Gamma_j$ .

Our proposed compact finite difference scheme attains the maximum overall accuracy order everywhere on the domain with the shortest stencil support for the problem (1.1)-(1.3). Similar to [14, 15], our approach is based on a critical observation regarding the inter-dependence of high order derivatives of the underlying solution. When constructing a discretization stencil, we start with a general expression that allows us to recover all possible sixth order finite difference schemes. Then, we determine the remaining free parameters in the stencil by using our new pollution minimization strategy that is based on the average truncation error of plane waves. Our method differs from existing dispersion minimization methods in the literature in several ways. First, our method does not require us to compute the numerical wavenumber. Second, we use our pollution minimization procedure in the construction of all interior, boundary, and corner stencils. This is in stark contrast to the common approach in the literature, where the dispersion is minimized only in the interior stencil. The effectiveness of our pollution minimization strategy is evident from our numerical experiments. Our proposed compact finite difference scheme with reduced pollution effect outperforms several state-of-the-art finite difference schemes in the literature, particularly in the pre-asymptotic critical region where  $kh$  is near 1. When a large wavenumber  $k$  is present, this means that our proposed finite difference scheme is more accurate than others at a computationally feasible grid size.

We provide a comprehensive treatment of mixed inhomogeneous boundary conditions. In particular, our approach is capable of handling all possible combinations of Dirichlet, Neumann, and impedance boundary conditions for the 2D Helmholtz equation defined on a rectangular domain. For each corner, we explicitly provide a 4-point stencil with at least sixth order accuracy and reduced pollution effect. For each side, we explicitly give a 6-point stencil with at least sixth order accuracy and reduced pollution effect. To the best of our knowledge, our present work is the first paper to

comprehensively study the construction of corner and boundary finite difference stencils for all possible combinations of boundary conditions on a rectangular domain. Unlike the common technique used in the literature, no ghost or artificial points are introduced in our construction.

For the Helmholtz interface problem in (1.1), we derive a seventh order compact finite difference scheme to handle nonzero jump functions at the interface. I.e., such a scheme is used at an irregular point near the interface  $\Gamma_I$ ; the stencil centered at this point overlaps with both  $\Omega^+$  and  $\Omega^-$  subregions.

Since our proposed finite difference scheme is compact, the linear system arising from the discretization is sparse. The stencils themselves have a nice structure in that their coefficients are symmetric and take the form of polynomials of  $kh$ . Also, the coefficients in our interior stencil are simpler compared to [8], as they are polynomials of degree 6, while those in [8] are of degree 16. Hence, the process of assembling the coefficient matrix is highly efficient. Furthermore, for a fixed wavenumber  $k$  and for any given interface and boundary data, the coefficient matrix of our linear system does not change; only the vector on the right-hand side of the linear system changes.

The organization of this paper is as follows. In Section 2, we explain how our proposed sixth order compact finite difference scheme with reduced pollution effect is developed. We start our discussion by constructing the interior finite difference stencil with reduced pollution. Second, we construct the sixth order boundary and corner finite difference stencils with reduced pollution. Third, we construct the compact interface finite difference stencil. In Section 3, we present several numerical experiments to demonstrate the performance of our proposed sixth order compact finite difference scheme with reduced pollution effect. In Section 4, we present the proofs of several theorems stated in Section 2.

## 2. STENCILS FOR SIXTH ORDER COMPACT FINITE DIFFERENCE SCHEMES WITH REDUCED POLLUTION EFFECT USING UNIFORM CARTESIAN GRIDS

We follow the same setup as in [14, 15]. As stated in the introduction, let  $\Omega = (l_1, l_2) \times (l_3, l_4)$ . Without loss of generality, we assume  $l_4 - l_3 = N_0(l_2 - l_1)$  for some  $N_0 \in \mathbb{N}$ . For any positive integer  $N_1 \in \mathbb{N}$ , we define  $N_2 := N_0N_1$  and so the grid size is  $h := (l_2 - l_1)/N_1 = (l_4 - l_3)/N_2$ . Let

$$x_i = l_1 + ih, \quad i = 0, \dots, N_1, \quad \text{and} \quad y_j = l_3 + jh, \quad j = 0, \dots, N_2. \quad (2.1)$$

Our focus of this section is to develop sixth order compact finite difference schemes with reduced pollution effect on uniform Cartesian grids. Recall that a compact stencil centered at  $(x_i, y_j)$  contains nine points  $(x_i + kh, y_j + lh)$  for  $k, l \in \{-1, 0, 1\}$ . Define

$$\begin{aligned} d_{i,j}^+ &:= \{(k, \ell) : k, \ell \in \{-1, 0, 1\}, \psi(x_i + kh, y_j + \ell h) \geq 0\}, \quad \text{and} \\ d_{i,j}^- &:= \{(k, \ell) : k, \ell \in \{-1, 0, 1\}, \psi(x_i + kh, y_j + \ell h) < 0\}. \end{aligned}$$

Thus, the interface curve  $\Gamma_I := \{(x, y) \in \Omega : \psi(x, y) = 0\}$  splits the nine points in our compact stencil into two disjoint sets  $\{(x_{i+k}, y_{j+\ell}) : (k, \ell) \in d_{i,j}^+\} \subseteq \Omega^+ \cup \Gamma_I$  and  $\{(x_{i+k}, y_{j+\ell}) : (k, \ell) \in d_{i,j}^-\} \subseteq \Omega^-$ . We refer to a grid/center point  $(x_i, y_j)$  as a *regular point* if  $d_{i,j}^+ = \emptyset$  or  $d_{i,j}^- = \emptyset$ . The center point  $(x_i, y_j)$  of a stencil is *regular* if all its nine points are completely in  $\Omega^+ \cup \Gamma_I$  (hence  $d_{i,j}^- = \emptyset$ ) or in  $\Omega^-$  (i.e.,  $d_{i,j}^+ = \emptyset$ ). Otherwise, the center point  $(x_i, y_j)$  of a stencil is referred to as *an irregular point* if both  $d_{i,j}^+$  and  $d_{i,j}^-$  are nonempty.

Now, let us pick and fix a base point  $(x_i^*, y_j^*)$  inside the open square  $(x_i - h, x_i + h) \times (y_j - h, y_j + h)$ , which can be written as

$$x_i^* = x_i - v_0h \quad \text{and} \quad y_j^* = y_j - w_0h \quad \text{with} \quad -1 < v_0, w_0 < 1. \quad (2.2)$$

We shall use the following notations:

$$u^{(m,n)} := \frac{\partial^{m+n} u}{\partial^m x \partial^n y}(x_i^*, y_j^*) \quad \text{and} \quad f^{(m,n)} := \frac{\partial^{m+n} f}{\partial^m x \partial^n y}(x_i^*, y_j^*), \quad (2.3)$$

which are used to represent their  $(m, n)$ th partial derivatives at the base point  $(x_i^*, y_j^*)$ . Define  $\mathbb{N}_0 := \mathbb{N} \cup \{0\}$ , the set of all nonnegative integers. Given  $L \in \mathbb{N}_0$ , we define

$$\Lambda_L := \{(m, n - m) : n = 0, \dots, L \text{ and } m = 0, \dots, n\}, \quad L \in \mathbb{N}_0. \quad (2.4)$$

For a smooth function  $u$  and small  $x, y$ , the values  $u(x + x_i^*, y + y_j^*)$  are well approximated by its Taylor polynomial as follows:

$$u(x + x_i^*, y + y_j^*) = \sum_{(m,n) \in \Lambda_{M+1}} \frac{u^{(m,n)}}{m!n!} x^m y^n + \mathcal{O}(h^{M+2}), \quad x, y \in (-2h, 2h). \quad (2.5)$$

To put differently, in a neighborhood of the base point  $(x_i^*, y_j^*)$ , the function  $u$  is well approximated and completely determined by the partial derivatives of  $u$  of total degree less than  $M + 2$  at the base point  $(x_i^*, y_j^*)$ , i.e., by the unknown quantities  $u^{(m,n)}$ ,  $(m, n) \in \Lambda_{M+1}$ . The same holds for  $f(x + x_i^*, y + y_j^*)$ . For  $x \in \mathbb{R}$ , the floor function  $\lfloor x \rfloor$  is defined to be the largest integer less than or equal to  $x$ . For an integer  $m$ , we define

$$\text{odd}(m) := \frac{1 - (-1)^m}{2} = \begin{cases} 0, & \text{if } m \text{ is even,} \\ 1, & \text{if } m \text{ is odd.} \end{cases}$$

Since the function  $u$  is a solution to the partial differential equation in (1.1), all quantities  $u^{(m,n)}$ ,  $(m, n) \in \Lambda_{M+1}$  are not independent of each other. The next lemma describes this dependence.

**Lemma 2.1.** *Let  $u$  be a smooth function satisfying  $\Delta u + k^2 u = f$  in  $\Omega \setminus \Gamma_I$ . If a point  $(x_i^*, y_j^*) \in \Omega \setminus \Gamma_I$ , then*

$$u^{(m,n)} = (-1)^{\lfloor \frac{m}{2} \rfloor} \sum_{i=0}^{\lfloor \frac{m}{2} \rfloor} \binom{\lfloor \frac{m}{2} \rfloor}{i} k^{2i} u^{(\text{odd}(m), 2\lfloor \frac{m}{2} \rfloor + n - 2i)} + \sum_{i=1}^{\lfloor \frac{m}{2} \rfloor} \sum_{j=0}^{i-1} (-1)^{i-1} \binom{i-1}{j} k^{2(i-j-1)} f^{(m-2i, n+2j)} \quad (2.6)$$

for all  $(m, n) \in \Lambda_{M+1}^{V,2}$ , where

$$\Lambda_{M+1}^{V,2} := \Lambda_{M+1} \setminus \Lambda_{M+1}^{V,1} \quad \text{with} \quad \Lambda_{M+1}^{V,1} := \{(\ell, k - \ell) : k = \ell, \dots, M + 1 - \ell \text{ and } \ell = 0, 1\}. \quad (2.7)$$

Define

$$\Lambda_{M+1}^{H,j} := \{(n, m) : (m, n) \in \Lambda_{M+1}^{V,j}, j = 1, 2\}.$$

If a point  $(x_i^*, y_j^*) \in \Omega \setminus \Gamma_I$ , then

$$u^{(m,n)} = (-1)^{\lfloor \frac{n}{2} \rfloor} \sum_{i=0}^{\lfloor \frac{n}{2} \rfloor} \binom{\lfloor \frac{n}{2} \rfloor}{i} k^{2i} u^{(2\lfloor \frac{n}{2} \rfloor + m - 2i, \text{odd}(n))} + \sum_{i=1}^{\lfloor \frac{n}{2} \rfloor} \sum_{j=0}^{i-1} (-1)^{i-1} \binom{i-1}{j} k^{2(i-j-1)} f^{(m+2j, n-2i)} \quad (2.8)$$

for all  $(m, n) \in \Lambda_{M+1}^{H,2}$ .

*Proof.* The proof is similar to the proof of [14, Lemma 2.1] and [15, Lemma 2.1].  $\square$

See [14, Figure 6] for an illustration of how each  $u^{(m,n)}$  with  $(m, n) \in \Lambda_7$  is categorized based on  $\Lambda_7^{V,j}$  with  $j \in \{1, 2\}$ . From (2.6), we have

$$\begin{aligned} \sum_{(m,n) \in \Lambda_{M+1}^{V,2}} \frac{x^m y^n}{m!n!} u^{(m,n)} &= \overbrace{\sum_{(m,n) \in \Lambda_{M+1}^{V,2}} \frac{x^m y^n}{m!n!} \left\{ (-1)^{\lfloor \frac{m}{2} \rfloor} \sum_{i=0}^{\lfloor \frac{m}{2} \rfloor} \binom{\lfloor \frac{m}{2} \rfloor}{i} k^{2i} u^{(\text{odd}(m), 2\lfloor \frac{m}{2} \rfloor + n - 2i)} \right\}}^{=: I_1} \\ &+ \underbrace{\sum_{(m,n) \in \Lambda_{M+1}^{V,2}} \frac{x^m y^n}{m!n!} \left\{ \sum_{i=1}^{\lfloor \frac{m}{2} \rfloor} \sum_{j=0}^{i-1} (-1)^{i-1} \binom{i-1}{j} k^{2i-2j-2} f^{(m-2i, n+2j)} \right\}}_{=: I_2}, \end{aligned} \quad (2.9)$$

where the first summation  $I_1$  above can be expressed as

$$I_1 = \sum_{\substack{(m,n) \in \Lambda_{M+1}^{V,2} \\ \ell = \frac{m}{2}, \text{ even } m}} \frac{(-1)^\ell x^{2\ell} y^n}{(2\ell)!n!} \sum_{i=0}^{\ell} \binom{\ell}{i} k^{2i} u^{(0, 2\ell + n - 2i)} + \sum_{\substack{(m,n) \in \Lambda_{M+1}^{V,2} \\ \ell = \frac{m-1}{2}, \text{ odd } m}} \frac{(-1)^\ell x^{2\ell+1} y^n}{(2\ell+1)!n!} \sum_{i=0}^{\ell} \binom{\ell}{i} k^{2i} u^{(1, 2\ell + n - 2i)}$$

$$\begin{aligned}
&= \sum_{n=2}^{M+1} \sum_{\ell=1}^{\lfloor \frac{n}{2} \rfloor} \frac{(-1)^\ell x^{2\ell} y^{n-2\ell}}{(2\ell)!(n-2\ell)!} \sum_{i=0}^{\ell} \binom{\ell}{i} k^{2i} u^{(0,n-2i)} + \sum_{n=2}^M \sum_{\ell=1}^{\lfloor \frac{n}{2} \rfloor} \frac{(-1)^\ell x^{2\ell+1} y^{n-2\ell}}{(2\ell+1)!(n-2\ell)!} \sum_{i=0}^{\ell} \binom{\ell}{i} k^{2i} u^{(1,n-2i)} \\
&= \sum_{\substack{(m,n) \in \Lambda_{M+1}^{V,1} \\ n \geq 2}} \sum_{\ell=1}^{\lfloor \frac{n}{2} \rfloor} \frac{(-1)^\ell x^{m+2\ell} y^{n-2\ell}}{(m+2\ell)!(n-2\ell)!} \sum_{i=0}^{\ell} \binom{\ell}{i} k^{2i} u^{(m,n-2i)},
\end{aligned}$$

and the second summation  $I_2$  above can be expressed as

$$\begin{aligned}
I_2 &= \sum_{(m,n) \in \Lambda_{M-1}} \sum_{\ell=1}^{1+\lfloor \frac{n}{2} \rfloor} \sum_{p=0}^{\ell-1} (-1)^{\ell-1} \binom{\ell-1}{p} k^{2(\ell-p-1)} f^{(m,n+2(p+1-\ell))} \frac{x^{m+2\ell} y^{n-2\ell+2}}{(m+2\ell)!(n-2\ell+2)!} \\
&= \sum_{(m,n) \in \Lambda_{M-1}} \sum_{\substack{j \in \{n+2p \mid p \in \mathbb{N}_0, \\ n+2p \leq M+1-m\}}} \sum_{\ell=1+\lfloor \frac{j-n}{2} \rfloor}^{1+\lfloor \frac{j}{2} \rfloor} (-1)^{\ell-1} \binom{\ell-1}{\frac{j-n}{2}} k^{j-n} \frac{x^{m+2\ell} y^{j-2\ell+2}}{(m+2\ell)!(j-2\ell+2)!} f^{(m,n)} \\
&= \sum_{(m,n) \in \Lambda_{M-1}} \underbrace{\sum_{p=0}^{\lfloor \frac{M+1-m-n}{2} \rfloor} \sum_{\ell=1+p}^{1+\lfloor p+\frac{n}{2} \rfloor} (-1)^{\ell-1} \binom{\ell-1}{p} k^{2p} \frac{x^{m+2\ell} y^{2p+n+2-2\ell}}{(m+2\ell)!(2p+n+2-2\ell)!} f^{(m,n)}}_{=: Q_{M,m,n}^V(x,y)}.
\end{aligned} \tag{2.10}$$

Hence, using the right-hand side of (2.5) and the definitions of  $\Lambda_{M+1}^{V,1}$ ,  $\Lambda_{M+1}^{V,2}$  in (2.7), we have

$$\begin{aligned}
I_1 + \sum_{(m,n) \in \Lambda_{M+1}^{V,1}} \frac{x^m y^n}{m!n!} u^{(m,n)} &= \sum_{(m,n) \in \Lambda_{M+1}^{V,1}} \sum_{i=0}^{\lfloor \frac{n}{2} \rfloor} \sum_{\ell=i}^{\lfloor \frac{n}{2} \rfloor} \frac{(-1)^\ell x^{m+2\ell} y^{n-2\ell}}{(m+2\ell)!(n-2\ell)!} \binom{\ell}{i} k^{2i} u^{(m,n-2i)} \\
&= \sum_{(m,n) \in \Lambda_{M+1}^{V,1}} \sum_{\substack{i \in \{n+2p \mid p \in \mathbb{N}_0, \\ n+2p \leq M+1-m\}}} \sum_{\ell=\frac{i-n}{2}}^{\lfloor \frac{i}{2} \rfloor} \frac{(-1)^\ell x^{m+2\ell} y^{i-2\ell}}{(m+2\ell)!(i-2\ell)!} \binom{\ell}{\frac{i-n}{2}} k^{i-n} u^{(m,n)} \\
&= \sum_{(m,n) \in \Lambda_{M+1}^{V,1}} \underbrace{\sum_{p=0}^{\lfloor \frac{M+1-m-n}{2} \rfloor} \sum_{\ell=p}^{p+\lfloor \frac{n}{2} \rfloor} \frac{(-1)^\ell x^{m+2\ell} y^{n+2p-2\ell}}{(m+2\ell)!(n+2p-2\ell)!} \binom{\ell}{p} k^{2p} u^{(m,n)}}_{=: G_{M,m,n}^V(x,y)}.
\end{aligned} \tag{2.11}$$

Suppose  $x, y \in (-2h, 2h)$ . The lowest degree of  $h$  for each polynomial  $G_{M,m,n}^V(x, y)$  with  $(m, n) \in \Lambda_{M+1}^{V,1}$  in (2.11) is  $m+n$ . The lowest degree of  $h$  for each polynomial  $Q_{M,m,n}^V(x, y)$  with  $(m, n) \in \Lambda_{M-1}^{V,1}$  in (2.10) is  $m+n+2$ . Therefore, by (2.9)-(2.10), we can rewrite the approximation of  $u(x+x_i^*, y+y_j^*)$  with  $(x, y) \in (-2h, 2h)$  in (2.5) as follows:

$$u(x+x_i^*, y+y_j^*) = \sum_{(m,n) \in \Lambda_{M+1}^{V,1}} u^{(m,n)} G_{M,m,n}^V(x, y) + \sum_{(m,n) \in \Lambda_{M_f-1}} f^{(m,n)} Q_{M_f,m,n}^V(x, y) + \mathcal{O}(h^{M+2}), \tag{2.12}$$

where  $M, M_f \in \mathbb{N}_0$  and  $M_f \geq M$ . By a similar calculation, for  $(x, y) \in (-2h, 2h)$ , we also have

$$u(x+x_i^*, y+y_j^*) = \sum_{(m,n) \in \Lambda_{M+1}^{H,1}} u^{(m,n)} G_{M,m,n}^H(x, y) + \sum_{(m,n) \in \Lambda_{M_f-1}} f^{(m,n)} Q_{M_f,m,n}^H(x, y) + \mathcal{O}(h^{M+2}), \tag{2.13}$$

where  $M, M_f \in \mathbb{N}_0$ ,  $M_f \geq M$  and

$$\begin{aligned}
G_{M,m,n}^H(x, y) &:= G_{M,n,m}^V(y, x), \quad \text{for all } n \in \{0, 1\}, m \in \mathbb{N}_0 \\
Q_{M,m,n}^H(x, y) &:= Q_{M,n,m}^V(y, x), \quad \text{for all } m, n \in \mathbb{N}_0.
\end{aligned} \tag{2.14}$$

Identities (2.12)-(2.13) are critical in finding compact stencils achieving a desired accuracy order.

In the following subsections, we shall explicitly present our stencils having at least accuracy order 6 with reduced pollution effect for interior, boundary and corner points. As we shall explain in details in Section 4, we construct such stencils by first finding a general expression for all possible discretization stencils achieving the maximum order. Then we minimize the average truncation error of plane waves to determine the remaining free parameters in each stencil to reduce pollution effect.

**2.1. Regular points (interior).** In this subsection, we state one of our main results on a sixth order (which is the highest possible order) compact finite difference scheme (with reduced pollution effect) centered at a regular point  $(x_i, y_j)$  and  $(x_i, y_j) \notin \partial\Omega$ . We let  $(x_i, y_j)$  be the base point  $(x_i^*, y_j^*)$  by setting  $v_0 = w_0 = 0$  in (2.2). The proof of the following theorem is deferred to Section 4.

**Theorem 2.2.** *Let a grid point  $(x_i, y_j)$  be a regular point, i.e., either  $d_{i,j}^+ = \emptyset$  or  $d_{i,j}^- = \emptyset$  and  $(x_i, y_j) \notin \partial\Omega$ . Let  $(u_h)_{i,j}$  be the numerical approximated solution of the exact solution  $u$  of the Helmholtz equation (1.1) at an interior regular point  $(x_i, y_j)$ . Then the following discretization stencil centered at  $(x_i, y_j)$*

$$\begin{aligned} & C_{1,1}(u_h)_{i-1,j-1} + C_{1,0}(u_h)_{i,j-1} + C_{1,1}(u_h)_{i+1,j-1} \\ \mathcal{L}_h u_h := & +C_{1,0}(u_h)_{i-1,j} + C_{0,0}(u_h)_{i,j} + C_{1,0}(u_h)_{i+1,j} = \sum_{(m,n) \in \Lambda_6} f^{(m,n)} C_{f,m,n}, \\ & +C_{1,1}(u_h)_{i-1,j+1} + C_{1,0}(u_h)_{i,j+1} + C_{1,1}(u_h)_{i+1,j+1} \end{aligned} \quad (2.15)$$

achieves the sixth order accuracy for  $\Delta u + k^2 u = f$  at the point  $(x_i, y_j)$  with reduced pollution effect,

where  $C_{f,m,n} := \sum_{k=-1}^1 \sum_{\ell=-1}^1 C_{k,\ell} Q_{7,m,n}^V(kh, \ell h)$  for all  $(m, n) \in \Lambda_6$ ,  $Q_{7,m,n}^V(x, y)$  is defined in (2.10), and

$$\begin{aligned} C_{-1,-1} &= C_{-1,1} = C_{1,-1} = C_{1,1}, \quad C_{-1,0} = C_{0,-1} = C_{0,1} = C_{1,0}, \\ C_{1,1} &= 1 - \frac{357462387}{25 \times 10^{10}} kh + \frac{1001065991}{2 \times 10^{10}} (kh)^2 - \frac{196477327}{2 \times 10^{12}} (kh)^3 + \frac{1155977087}{10^{12}} (kh)^4 - \frac{116352513}{4 \times 10^{13}} (kh)^5 + \frac{1255955641}{10^{14}} (kh)^6, \\ C_{1,0} &= 4 - \frac{357462387}{625 \times 10^8} kh + \frac{532995477}{25 \times 10^{11}} (kh)^2 - \frac{267461861}{25 \times 10^{11}} (kh)^3 - \frac{288674231}{10^{11}} (kh)^4 + \frac{2179972749}{5 \times 10^{14}} (kh)^5 - \frac{3473210401}{5 \times 10^{13}} (kh)^6, \\ C_{0,0} &= -20 + \frac{357462387}{125 \times 10^8} kh + \frac{5798934009}{10^9} (kh)^2 - \frac{969775457}{125 \times 10^9} (kh)^3 - \frac{1963785709}{5 \times 10^9} (kh)^4 + \frac{4056581719}{10^{13}} (kh)^5 + \frac{795951403}{10^{11}} (kh)^6. \end{aligned} \quad (2.16)$$

Moreover, the maximum accuracy order of a compact finite difference scheme for  $\Delta u + k^2 u = f$  at the point  $(x_i, y_j)$  is six.

**2.2. Boundary and corner points.** In this subsection, we discuss how to find a compact finite difference scheme centered at  $(x_i, y_j) \in \partial\Omega$ .

**2.2.1. Boundary points.** We first discuss in detail how the left boundary (i.e.,  $(x_i, y_j) \in \Gamma_1 = \{l_1\} \times (l_3, l_4)$ ) stencil is constructed. The stencils for the other three boundaries can afterwards be obtained by symmetry. If  $\mathcal{B}_1 u = u = g_1$  on  $\Gamma_1$ , then the left boundary stencil can be directly obtained from (2.15)-(2.16) in Theorem 2.2 by replacing  $(u_h)_{0,j-1}$ ,  $(u_h)_{0,j}$ , and  $(u_h)_{0,j+1}$  with  $g_1(y_{j-1})$ ,  $g_1(y_j)$ , and  $g_1(y_{j+1})$  respectively, where  $y_j \in (l_3, l_4)$ , and moving terms involving these known boundary values to the right-hand side of (2.15). The other three boundary sides are dealt in a similar straightforward fashion if a Dirichlet boundary condition is present. On the other hand, the stencils for the other two boundary conditions are not trivial at all. The following theorem provides the explicit 6-point stencil of accuracy order at least six with reduced pollution effect for the left boundary operator  $\mathcal{B}_1 \in \{\frac{\partial}{\partial \bar{n}} - i\mathbf{k}\mathbf{I}_d, \frac{\partial}{\partial \bar{n}}\}$ . The proof of the following result is deferred to Section 4.

**Theorem 2.3.** *Assume  $\Omega = (l_1, l_2) \times (l_3, l_4)$ . Let  $(u_h)_{i,j}$  be the numerical approximated solution of the exact solution  $u$  of the Helmholtz equation (1.1) at the point  $(x_i, y_j)$ . Consider the following discretization stencil centered at  $(x_0, y_j) \in \Gamma_1$  for  $\mathcal{B}_1 u = g_1$  on  $\Gamma_1$  with  $\mathcal{B}_1 \in \{\frac{\partial}{\partial \bar{n}} - i\mathbf{k}\mathbf{I}_d, \frac{\partial}{\partial \bar{n}}\}$ :*

$$\begin{aligned} & C_{0,1}^{\mathcal{B}_1}(u_h)_{0,j-1} + C_{1,1}^{\mathcal{B}_1}(u_h)_{1,j-1} \\ \mathcal{L}_h^{\mathcal{B}_1} u_h := & +C_{0,0}^{\mathcal{B}_1}(u_h)_{0,j} + C_{1,0}^{\mathcal{B}_1}(u_h)_{1,j} = \sum_{(m,n) \in \Lambda_6} f^{(m,n)} C_{f,m,n}^{\mathcal{B}_1} + \sum_{n=0}^7 g_1^{(n)} C_{g_1,n}^{\mathcal{B}_1}, \\ & +C_{0,1}^{\mathcal{B}_1}(u_h)_{0,j+1} + C_{1,1}^{\mathcal{B}_1}(u_h)_{1,j+1} \end{aligned} \quad (2.17)$$

where  $\{C_{k,\ell}^{\mathcal{B}_1}\}_{k \in \{0,1\}, \ell \in \{-1,0,1\}}$  are polynomials of  $kh$ ,  $C_{f,m,n}^{\mathcal{B}_1} = \sum_{k=0}^1 \sum_{\ell=-1}^1 C_{k,\ell}^{\mathcal{B}_1} Q_{7,m,n}^V(kh, \ell h)$  for all  $(m, n) \in \Lambda_6$ ,  $Q_{7,m,n}^V$  is defined in (2.10),  $g_1^{(n)} := \frac{d^n g_1}{dy^n}(y_j)$ ,  $C_{g_1,n}^{\mathcal{B}_1} = -\sum_{k=0}^1 \sum_{\ell=-1}^1 C_{k,\ell}^{\mathcal{B}_1} G_{7,1,n}^V(kh, \ell h)$  for all  $n = 0, \dots, 7$ ,  $G_{7,1,n}^V$  is defined in (2.11),  $C_{0,-1}^{\mathcal{B}_1} = C_{0,1}^{\mathcal{B}_1}$ , and  $C_{1,-1}^{\mathcal{B}_1} = C_{1,1}^{\mathcal{B}_1}$ .

(1) For  $\mathcal{B}_1 = \frac{\partial}{\partial \bar{n}} - i\mathbf{kI}_d$ , the coefficients for defining  $\mathcal{L}_h^{\mathcal{B}_1} u_h$  in (2.17) are given by

$$\begin{aligned} C_{1,1}^{\mathcal{B}_1} &= 1 - \frac{218737123}{10^9} kh + \frac{6698622893i}{10^{10}} kh - \frac{1620223367}{10^{10}} (kh)^2 - \frac{1202725989i}{10^{10}} (kh)^2 + \frac{3105005559}{10^{11}} (kh)^3 - \frac{1252107029i}{10^{11}} (kh)^3 \\ &\quad - \frac{3412232989}{10^{12}} (kh)^4 - \frac{1505046263i}{10^{12}} (kh)^4, \\ C_{0,1}^{\mathcal{B}_1} &= 2 - \frac{218737123}{5 \times 10^8} kh + \frac{1139724579i}{10^9} kh - \frac{3034055489}{10^{10}} (kh)^2 - \frac{1967977733i}{10^{10}} (kh)^2 + \frac{1090897501}{25 \times 10^9} (kh)^3 - \frac{7785677273i}{10^{11}} (kh)^3 \\ &\quad + \frac{98544681}{4 \times 10^9} (kh)^4 + \frac{1218033221i}{5 \times 10^{10}} (kh)^4, \\ C_{1,0}^{\mathcal{B}_1} &= 4 - \frac{8749484921}{10^{10}} kh + \frac{2279449157i}{10^9} kh - \frac{946955529}{2 \times 10^9} (kh)^2 - \frac{1967977733i}{5 \times 10^9} (kh)^2 + \frac{2905342517}{5 \times 10^{10}} (kh)^3 - \frac{1542150899i}{5 \times 10^{10}} (kh)^3 \\ &\quad + \frac{2645544603}{10^{12}} (kh)^4 + \frac{302693249i}{25 \times 10^9} (kh)^4, \\ C_{0,0}^{\mathcal{B}_1} &= -10 + \frac{218737123}{10^8} kh + \frac{202754213i}{2 \times 10^9} kh + \frac{7851597997}{10^{10}} (kh)^2 - \frac{2846864471i}{10^{10}} (kh)^2 - \frac{1147746931}{5 \times 10^9} (kh)^3 + \frac{2236631341i}{10^{10}} (kh)^3 \\ &\quad - \frac{1738692843}{5 \times 10^{10}} (kh)^4 - \frac{898631349i}{25 \times 10^9} (kh)^4. \end{aligned} \tag{2.18}$$

Then the finite difference scheme in (2.17) achieves sixth order accuracy for  $\mathcal{B}_1 u = \frac{\partial u}{\partial \bar{n}} - iku = g_1$  at the point  $(x_0, y_j) \in \Gamma_1$  with reduced pollution effect. The maximum accuracy order of a 6-point finite difference scheme for  $\mathcal{B}_1 u = \frac{\partial u}{\partial \bar{n}} - iku = g_1$  at the point  $(x_0, y_j) \in \Gamma_1$  is six.

(2) For  $\mathcal{B}_1 = \frac{\partial}{\partial \bar{n}}$ , the coefficients for defining  $\mathcal{L}_h^{\mathcal{B}_1} u_h$  in (2.17) are given by

$$\begin{aligned} C_{1,1}^{\mathcal{B}_1} &= 1 + \frac{1915061419}{25 \times 10^9} (kh)^2 + \frac{3019639439}{10^{12}} (kh)^4, & C_{0,1}^{\mathcal{B}_1} &= 2 + \frac{665061419}{125 \times 10^8} (kh)^2 - \frac{1071383831}{2 \times 10^{12}} (kh)^4, \\ C_{1,0}^{\mathcal{B}_1} &= 4 + \frac{106409827}{10^9} (kh)^2 - \frac{1071383831}{10^{12}} (kh)^4, & C_{0,0}^{\mathcal{B}_1} &= -10 + \frac{1316987716}{5 \times 10^8} (kh)^2 - \frac{1240891409}{10^{10}} (kh)^4. \end{aligned} \tag{2.19}$$

Then the finite difference scheme in (2.17) achieves seventh order accuracy for  $\mathcal{B}_1 u = \frac{\partial u}{\partial \bar{n}} = g_1$  at the point  $(x_0, y_j) \in \Gamma_1$  with reduced pollution effect. Moreover, the maximum accuracy order of a 6-point finite difference scheme for  $\mathcal{B}_1 u = \frac{\partial u}{\partial \bar{n}} = g_1$  at the point  $(x_0, y_j) \in \Gamma_1$  is seven.

By symmetry, we can immediately state the stencils for the other three boundary sides. Same accuracy order results as in Theorem 2.3 hold. First, consider the following discretization stencil for  $\mathcal{B}_2 u = g_2$  on  $\Gamma_2$  with  $\mathcal{B}_2 \in \{\frac{\partial}{\partial \bar{n}} - i\mathbf{kI}_d, \frac{\partial}{\partial \bar{n}}\}$  centered at  $(x_{N_1}, y_j) \in \Gamma_2$ :

$$\mathcal{L}_h^{\mathcal{B}_2} u_h := \sum_{k=-1}^0 \sum_{\ell=-1}^1 C_{k,\ell}^{\mathcal{B}_2} (u_h)_{N_1+k,j+\ell} = \sum_{(m,n) \in \Lambda_6} f^{(m,n)} C_{f,m,n}^{\mathcal{B}_2} + \sum_{n=0}^7 g_2^{(n)} C_{g_2,n}^{\mathcal{B}_2},$$

where  $C_{-k,\ell}^{\mathcal{B}_2} = C_{k,\ell}^{\mathcal{B}_1}$  for all  $k \in \{0,1\}$ ,  $\ell \in \{-1,0,1\}$ ,  $C_{f,m,n}^{\mathcal{B}_2} = \sum_{k=-1}^0 \sum_{\ell=-1}^1 Q_{7,m,n}^V(kh, \ell h)$  for all  $(m, n) \in \Lambda_6$ ,  $g_2^{(n)} := \frac{d^n g_2}{dy^n}(y_j)$ ,  $C_{g_2,n}^{\mathcal{B}_2} = \sum_{k=-1}^0 \sum_{\ell=-1}^1 C_{k,\ell}^{\mathcal{B}_2} G_{7,1,n}^V(kh, \ell h)$  for all  $n = 0, \dots, 7$ .

Second, the stencil for  $\mathcal{B}_3 u = g_3$  on  $\Gamma_3$  with  $\mathcal{B}_3 \in \{\frac{\partial}{\partial \bar{n}} - i\mathbf{kI}_d, \frac{\partial}{\partial \bar{n}}\}$  centered at  $(x_i, y_0) \in \Gamma_3$  is

$$\mathcal{L}_h^{\mathcal{B}_3} u_h := \sum_{k=-1}^1 \sum_{\ell=0}^1 C_{k,\ell}^{\mathcal{B}_3} (u_h)_{i+k,\ell} = \sum_{(m,n) \in \Lambda_6} f^{(m,n)} C_{f,m,n}^{\mathcal{B}_3} + \sum_{n=0}^7 g_3^{(n)} C_{g_3,n}^{\mathcal{B}_3},$$

where  $C_{\ell,k}^{\mathcal{B}_3} = C_{k,\ell}^{\mathcal{B}_1}$  for all  $k \in \{0,1\}$ ,  $\ell \in \{-1,0,1\}$ ,  $C_{f,m,n}^{\mathcal{B}_3} = \sum_{k=-1}^1 \sum_{\ell=0}^1 C_{k,\ell}^{\mathcal{B}_3} Q_{7,m,n}^H(kh, \ell h)$  for all  $(m, n) \in \Lambda_6$ ,  $Q_{7,m,n}^H$  is defined in (2.14),  $g_3^{(n)} := \frac{d^n g_3}{dx^n}(x_i)$ ,  $C_{g_3,n}^{\mathcal{B}_3} = -\sum_{k=-1}^1 \sum_{\ell=0}^1 C_{k,\ell}^{\mathcal{B}_3} G_{7,n,1}^H(kh, \ell h)$  for all  $n = 0, \dots, 7$ , and  $G_{7,n,1}^H$  is defined in (2.14).



Third, the stencil for  $\mathcal{B}_4 u = g_4$  on  $\Gamma_4$  with  $\mathcal{B}_4 \in \left\{ \frac{\partial}{\partial \bar{n}} - ik\mathbf{I}_d, \frac{\partial}{\partial \bar{n}} \right\}$  centered at  $(x_i, y_{N_2}) \in \Gamma_4$  is

$$\mathcal{L}_h^{\mathcal{B}_4} u_h := \sum_{k=-1}^1 \sum_{\ell=-1}^0 C_{k,\ell}^{\mathcal{B}_4} (u_h)_{i+k, N_2+\ell} = \sum_{(m,n) \in \Lambda_6} f^{(m,n)} C_{f,m,n}^{\mathcal{B}_4} + \sum_{n=0}^7 g_4^{(n)} C_{g_4,n}^{\mathcal{B}_4},$$

where  $C_{\ell,-k}^{\mathcal{B}_4} = C_{k,\ell}^{\mathcal{B}_1}$  for all  $k \in \{0, 1\}$ ,  $\ell \in \{-1, 0, 1\}$ ,  $C_{f,m,n}^{\mathcal{B}_4} = \sum_{k=-1}^1 \sum_{\ell=-1}^0 C_{k,\ell}^{\mathcal{B}_4} Q_{7,m,n}^H(kh, \ell h)$  for all  $(m, n) \in \Lambda_6$ ,  $g_4^{(n)} := \frac{d^n g_4}{dx^n}(x_i)$ , and  $C_{g_4,n}^{\mathcal{B}_4} = \sum_{k=-1}^1 \sum_{\ell=-1}^0 C_{k,\ell}^{\mathcal{B}_4} G_{7,n,1}^H(kh, \ell h)$  for all  $n = 0, \dots, 7$ .

2.2.2. *Corner points.* For clarity of presentation, let us consider the following boundary configuration

$$\begin{aligned} \mathcal{B}_1 u &= \frac{\partial u}{\partial \bar{n}} - iku = g_1 \quad \text{on } \Gamma_1, & \mathcal{B}_2 u &= u = g_2 \quad \text{on } \Gamma_2, \\ \mathcal{B}_3 u &= \frac{\partial u}{\partial \bar{n}} = g_3 \quad \text{on } \Gamma_3, & \mathcal{B}_4 u &= \frac{\partial u}{\partial \bar{n}} - iku = g_4 \quad \text{on } \Gamma_4. \end{aligned} \quad (2.20)$$

See Fig. 1 for an illustration.

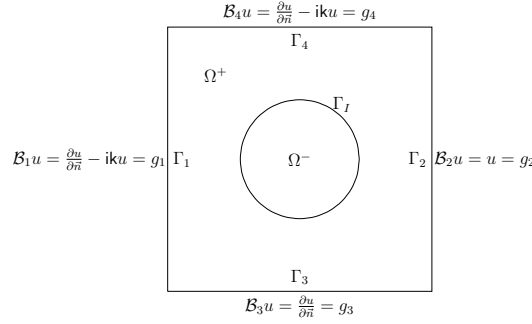


FIGURE 1. An illustration for the boundary configuration in (2.20), where  $\psi(x, y) = x^2 + y^2 - 2$ .

The corners coming from other boundary configurations can be handled in a similar way. When a corner involves at least one Dirichlet boundary condition, we can use Theorem 2.3 and subsequent remarks to handle it. We denote the bottom left corner (the intersection of  $\Gamma_1$  and  $\Gamma_3$ ) by  $\mathcal{R}_1$ , and the top left corner (the intersection of  $\Gamma_1$  and  $\Gamma_4$ ) by  $\mathcal{R}_2$ . In what follows, we discuss in detail how the bottom and top left stencils are constructed. The following two theorems provide the 4-point stencils of accuracy order at least six with reduced pollution effect for the left corners. Their proofs are deferred to Section 4.

**Theorem 2.4.** *Assume  $\Omega = (l_1, l_2) \times (l_3, l_4)$ . Let  $(u_h)_{i,j}$  be the numerical approximated solution of the exact solution  $u$  of the Helmholtz equation (1.1) at the point  $(x_i, y_j)$ . Then the following discretization stencil centered at the corner point  $(x_0, y_0)$ :*

$$\mathcal{L}_h^{\mathcal{R}_1} u_h := \begin{array}{l} C_{0,0}^{\mathcal{R}_1} (u_h)_{0,0} + C_{1,0}^{\mathcal{R}_1} (u_h)_{1,0} \\ + C_{0,1}^{\mathcal{R}_1} (u_h)_{0,1} + C_{1,1}^{\mathcal{R}_1} (u_h)_{1,1} \end{array} = \sum_{(m,n) \in \Lambda_6} f^{(m,n)} C_{f,m,n}^{\mathcal{R}_1} + \sum_{n=0}^7 g_1^{(n)} C_{g_1,n}^{\mathcal{R}_1} + \sum_{n=0}^7 g_3^{(n)} C_{g_3,n}^{\mathcal{R}_1}, \quad (2.21)$$

where

$$\begin{aligned} C_{1,1}^{\mathcal{R}_1} &= 1 - \frac{2041589737}{10^{10}} kh + \frac{6666011379i}{10^{10}} kh - \frac{1213438849}{10^{10}} (kh)^2 - \frac{254718888i}{25 \times 10^8} (kh)^2 + \frac{2199377569}{10^{11}} (kh)^3 + \frac{4307308979i}{5 \times 10^{11}} (kh)^3 \\ &\quad - \frac{5536966589}{10^{12}} (kh)^4 - \frac{1556373503i}{10^{12}} (kh)^4, \\ C_{1,0}^{\mathcal{R}_1} &= 2 - \frac{2041589737}{5 \times 10^9} kh + \frac{566601138i}{5 \times 10^8} kh - \frac{156034209}{10^9} (kh)^2 - \frac{1629433157i}{10^{10}} (kh)^2 + \frac{1855012159}{10^{11}} (kh)^3 + \frac{453336943i}{2 \times 10^{10}} (kh)^3 \\ &\quad - \frac{3170819689}{5 \times 10^{11}} (kh)^4 + \frac{25677723i}{8 \times 10^9} (kh)^4, \\ C_{0,1}^{\mathcal{R}_1} &= 2 - \frac{2041589737}{5 \times 10^9} kh + \frac{566601138i}{5 \times 10^8} kh - \frac{556752189}{25 \times 10^8} (kh)^2 - \frac{1629433157i}{10^{10}} (kh)^2 + \frac{3216071983}{10^{11}} (kh)^3 - \frac{3955100649i}{10^{11}} (kh)^3 \\ &\quad + \frac{1546871341}{10^{11}} (kh)^4 + \frac{231176972i}{125 \times 10^8} (kh)^4, \\ C_{0,0}^{\mathcal{R}_1} &= -5 + \frac{510397434}{5 \times 10^8} kh + \frac{6699431033i}{10^{11}} kh + \frac{2002755557}{10^{10}} (kh)^2 - \frac{369405469i}{2 \times 10^9} (kh)^2 - \frac{285280517}{25 \times 10^8} (kh)^3 + \frac{326982886i}{25 \times 10^8} (kh)^3 \\ &\quad + \frac{35165403}{25 \times 10^9} (kh)^4 - \frac{9939550949i}{10^{12}} (kh)^4, \end{aligned} \quad (2.22)$$

$g_1^{(n)} := \frac{d^n g_1}{dy^n}(y_0)$ ,  $g_3^{(n)} := \frac{d^n g_3}{dx^n}(x_0)$  for all  $n = 0, \dots, 7$ , and  $\{C_{f,m,n}^{\mathcal{R}_1}\}_{(m,n) \in \Lambda_6}$ ,  $\{C_{g_1,n}^{\mathcal{R}_1}\}_{n=0}^7$ ,  $\{C_{g_3,n}^{\mathcal{R}_1}\}_{n=0}^7$  are well-defined stencil coefficients that uniquely depend on  $\{C_{k,\ell}^{\mathcal{R}_1}\}_{k,\ell \in \{0,1\}}$ , achieves sixth order for  $\mathcal{B}_1 u = \frac{\partial u}{\partial \bar{n}} - iku = g_1$  and  $\mathcal{B}_3 u = \frac{\partial u}{\partial \bar{n}} = g_3$  at the point  $(x_0, y_0)$  with reduced pollution effect. Moreover, the maximum accuracy order of a 4-point finite difference scheme for  $\mathcal{B}_1 u = \frac{\partial u}{\partial \bar{n}} - iku = g_1$  and  $\mathcal{B}_3 u = \frac{\partial u}{\partial \bar{n}} = g_3$  at the point  $(x_0, y_0)$  is six.

**Theorem 2.5.** Assume  $\Omega = (l_1, l_2) \times (l_3, l_4)$ . Let  $(u_h)_{i,j}$  be the numerical approximated solution of the exact solution  $u$  of the Helmholtz equation (1.1) at the point  $(x_i, y_j)$ . Then the following discretization stencil centered at the corner point  $(x_0, y_{N_2})$ :

$$\mathcal{L}_h^{\mathcal{R}_2} u_h := \begin{array}{cc} C_{1,0}^{\mathcal{R}_2}(u_h)_{0,N_2-1} & + C_{1,-1}^{\mathcal{R}_2}(u_h)_{1,N_2-1} \\ + C_{0,0}^{\mathcal{R}_2}(u_h)_{0,N_2} & + C_{1,0}^{\mathcal{R}_2}(u_h)_{1,N_2} \end{array} = \sum_{(m,n) \in \Lambda_6} f^{(m,n)} C_{f,m,n}^{\mathcal{R}_2} + \sum_{n=0}^7 g_1^{(n)} C_{g_1,n}^{\mathcal{R}_2} + \sum_{n=0}^7 g_4^{(n)} C_{g_4,n}^{\mathcal{R}_2}, \quad (2.23)$$

where

$$\begin{aligned} C_{1,-1}^{\mathcal{R}_2} &= 1 - \frac{535927359}{5 \times 10^9} kh + \frac{131913924i}{10^8} kh - \frac{4650641357}{10^{10}} (kh)^2 - \frac{3255802571i}{10^{11}} (kh)^2 - \frac{1802358661}{10^{13}} (kh)^3 - \frac{137039551i}{25 \times 10^8} (kh)^3 \\ &\quad - \frac{116115549}{625 \times 10^8} (kh)^4 - \frac{390383949i}{2 \times 10^{11}} (kh)^4, \\ C_{1,0}^{\mathcal{R}_2} &= 2 - \frac{428741887}{2 \times 10^9} kh + \frac{2238278479i}{10^9} kh - \frac{5558059089}{10^{10}} (kh)^2 - \frac{278023284i}{125 \times 10^8} (kh)^2 + \frac{1525711827}{5 \times 10^{11}} (kh)^3 - \frac{57317954i}{5 \times 10^8} (kh)^3 \\ &\quad + \frac{2099795921}{10^{11}} (kh)^4 + \frac{1100929919i}{2 \times 10^{11}} (kh)^4, \\ C_{0,0}^{\mathcal{R}_2} &= -5 + \frac{1339818397}{25 \times 10^8} kh + \frac{2043038021i}{10^{10}} kh - \frac{1519079742}{5 \times 10^8} (kh)^2 - \frac{2830355397i}{5 \times 10^9} (kh)^2 - \frac{82143257}{5 \times 10^8} (kh)^3 + \frac{3401956461i}{10^{10}} (kh)^3, \\ &\quad + \frac{1420360677}{5 \times 10^9} (kh)^4 + \frac{4391249797i}{10^{11}} (kh)^4, \end{aligned} \quad (2.24)$$

$g_1^{(n)} := \frac{d^n g_1}{dy^n}(y_{N_2})$ ,  $g_4^{(n)} := \frac{d^n g_4}{dx^n}(x_0)$  for all  $n = 0, \dots, 7$ , and  $\{C_{f,m,n}^{\mathcal{R}_2}\}_{(m,n) \in \Lambda_6}$ ,  $\{C_{g_1,n}^{\mathcal{R}_2}\}_{n=0}^7$ ,  $\{C_{g_4,n}^{\mathcal{R}_2}\}_{n=0}^7$  are well-defined stencil coefficients that uniquely depend on  $\{C_{k,\ell}^{\mathcal{R}_2}\}_{k \in \{0,1\}, \ell \in \{-1,0\}}$  with  $C_{0,-1}^{\mathcal{R}_2} = C_{1,0}^{\mathcal{R}_2}$ , achieves seventh order accuracy for  $\mathcal{B}_1 u = \frac{\partial u}{\partial \bar{n}} - iku = g_1$  and  $\mathcal{B}_4 u = \frac{\partial u}{\partial \bar{n}} - iku = g_4$  at the point  $(x_0, y_{N_2})$  with reduced pollution effect. Moreover, the maximum accuracy order of a 4-point finite difference scheme for  $\mathcal{B}_1 u = \frac{\partial u}{\partial \bar{n}} - iku = g_1$  and  $\mathcal{B}_4 u = \frac{\partial u}{\partial \bar{n}} - iku = g_4$  at the point  $(x_0, y_{N_2})$  is seven.

Note that the right-hand sides of (2.21) and (2.23) can be explicitly recovered. See the proofs of Theorems 2.4 and 2.5 in Section 4 for details.

**2.3. Irregular points.** Let  $(x_i, y_j)$  be an irregular point (i.e., both  $d_{i,j}^+$  and  $d_{i,j}^-$  are nonempty) and let us take a base point  $(x_i^*, y_j^*) \in \Gamma_I \cap (x_i - h, x_i + h) \times (y_j - h, y_j + h)$  on the interface  $\Gamma_I$  and inside  $(x_i - h, x_i + h) \times (y_j - h, y_j + h)$ . By (2.2), we have

$$x_i^* = x_i - v_0 h \quad \text{and} \quad y_j^* = y_j - w_0 h \quad \text{with} \quad -1 < v_0, w_0 < 1 \quad \text{and} \quad (x_i^*, y_j^*) \in \Gamma_I. \quad (2.25)$$

Let  $u_{\pm}$  and  $f_{\pm}$  represent the solution  $u$  and source term  $f$  in  $\Omega^+$  or  $\Omega^-$ , respectively. Similar to (2.3), the following notations are used

$$\begin{aligned} u_{\pm}^{(m,n)} &:= \frac{\partial^{m+n} u_{\pm}}{\partial^m x \partial^n y}(x_i^*, y_j^*), & f_{\pm}^{(m,n)} &:= \frac{\partial^{m+n} f_{\pm}}{\partial^m x \partial^n y}(x_i^*, y_j^*), \\ g_D^{(m,n)} &:= \frac{\partial^{m+n} g_D}{\partial^m x \partial^n y}(x_i^*, y_j^*), & g_N^{(m,n)} &:= \frac{\partial^{m+n} g_N}{\partial^m x \partial^n y}(x_i^*, y_j^*). \end{aligned}$$

Since the interface curve  $\Gamma_I$  is smooth and the solution  $u$  and the source term  $f$  are assumed to be piecewise smooth, we can extend  $u_+$  and  $f_+$  on  $\Omega^+$  into smooth functions in a neighborhood of  $(x_i^*, y_j^*)$ . The same applies to  $u_-$  and  $f_-$  on  $\Omega^-$ . Identity similar to (2.12) still holds:

$$u_{\pm}(x + x_i^*, y + y_j^*) = \sum_{(m,n) \in \Lambda_{M+1}^{V,1}} u_{\pm}^{(m,n)} G_{M,m,n}^V(x, y) + \sum_{(m,n) \in \Lambda_{M_f-1}} f_{\pm}^{(m,n)} Q_{M_f,m,n}^V(x, y) + \mathcal{O}(h^{M+2}),$$

for  $x, y \in (-2h, 2h)$ , where  $\Lambda_{M+1}^{V,1}$  is defined in (2.7),  $\Lambda_{M_f-1}$  is defined in (2.4),  $G_{M,m,n}^V(x, y)$  is defined in (2.11),  $Q_{M_f,m,n}^V(x, y)$  is defined in (2.10). As in [14, 15], we assume that we have a parametric equation for  $\Gamma_I$  near the base point  $(x_i^*, y_j^*)$ . I.e.,

$$x = r(t) + x_i^*, \quad y = s(t) + y_j^*, \quad (r'(t))^2 + (s'(t))^2 > 0 \quad \text{for } t \in (-\epsilon, \epsilon) \quad \text{with } \epsilon > 0, \quad (2.26)$$

where  $r$  and  $s$  are smooth functions.

**Theorem 2.6.** *Let  $u$  be the solution to the Helmholtz interface problem in (1.1) and the base point  $(x_i^*, y_j^*) \in \Gamma_I$  be parameterized near  $(x_i^*, y_j^*)$  by (2.26). Then*

$$\begin{aligned} u_-^{(m',n')} &= u_+^{(m',n')} + \sum_{(m,n) \in \Lambda_{M-1}} \left( T_{m',n',m,n}^+ f_+^{(m,n)} + T_{m',n',m,n}^- f_-^{(m,n)} \right) + \sum_{(m,n) \in \Lambda_{M+1}} T_{m',n',m,n}^{gD} g_D^{(m,n)} \\ &+ \sum_{(m,n) \in \Lambda_M} T_{m',n',m,n}^{gN} g_N^{(m,n)}, \quad \forall (m', n') \in \Lambda_{M+1}^{V,1}, \end{aligned}$$

where all the transmission coefficients  $T^\pm, T^{gD}, T^{gN}$  are uniquely determined by  $r^{(k)}(0), s^{(k)}(0)$ , and  $k$  for  $k = 0, \dots, M+1$ .

*Proof.* The proof closely follows from the proof of [14, Theorem 2.3].  $\square$

Next, we state the compact finite difference stencil for interior irregular points.

**Theorem 2.7.** *Let  $(u_h)_{i,j}$  be the numerical solution of (1.1) at an interior irregular point  $(x_i, y_j)$ . Pick a base point  $(x_i^*, y_j^*)$  as in (2.25). Then the following compact scheme centered at the interior irregular point  $(x_i, y_j)$*

$$\begin{aligned} \mathcal{L}_h^{\Gamma_I} &:= +C_{1,1}(u_h)_{i-1,j-1} + C_{1,0}(u_h)_{i,j-1} + C_{1,1}(u_h)_{i+1,j-1} \\ &+ C_{1,0}(u_h)_{i-1,j} + C_{0,0}(u_h)_{i,j} + C_{1,0}(u_h)_{i+1,j} \\ &+ C_{1,1}(u_h)_{i-1,j+1} + C_{1,0}(u_h)_{i,j+1} + C_{1,1}(u_h)_{i+1,j+1} \\ &= \sum_{(m,n) \in \Lambda_6} f_+^{(m,n)} J_{m,n}^+ + \sum_{(m,n) \in \Lambda_6} f_-^{(m,n)} J_{m,n}^- + \sum_{(m,n) \in \Lambda_8} g_D^{(m,n)} J_{m,n}^{gD} + \sum_{(m,n) \in \Lambda_7} g_N^{(m,n)} J_{m,n}^{gN}, \end{aligned}$$

achieves seventh order accuracy, where  $\{C_{k,\ell}\}_{k,\ell \in \{-1,0,1\}}$  are defined in (2.16),  $J_{m,n}^\pm := J_{m,n}^{\pm,0} + J_{m,n}^{\pm,T}$  for all  $(m, n) \in \Lambda_6$ ,

$$\begin{aligned} J_{m,n}^{\pm,0} &:= \sum_{(k,\ell) \in d_{i,j}^\pm} C_{k,\ell} Q_{7,m,n}^V((v_0+k)h, (w_0+\ell)h), \quad J_{m,n}^{\pm,T} := \sum_{(m',n') \in \Lambda_8^{V,1}} I_{m',n'}^- T_{m',n',m,n}^\pm, \quad \forall (m,n) \in \Lambda_6, \\ J_{m,n}^{gD} &:= \sum_{(m',n') \in \Lambda_8^{V,1}} I_{m',n'}^- T_{m',n',m,n}^{gD}, \quad \forall (m,n) \in \Lambda_8, \quad J_{m,n}^{gN} := \sum_{(m',n') \in \Lambda_8^{V,1}} I_{m',n'}^- T_{m',n',m,n}^{gN}, \quad \forall (m,n) \in \Lambda_7, \\ I_{m,n}^- &:= \sum_{(k,\ell) \in d_{i,j}^-} C_{k,\ell} G_{7,m,n}^V((v_0+k)h, (w_0+\ell)h), \quad \forall (m,n) \in \Lambda_8^{V,1}. \end{aligned}$$

Moreover, the maximum accuracy order of a compact finite difference stencil for  $\Delta u + k^2 u = f$  at an interior irregular point  $(x_i, y_j)$  is seven.

*Proof.* The proof closely follows from the proof of [14, Theorem 2.4].  $\square$

### 3. NUMERICAL EXPERIMENTS

In this section, we let  $\Omega = (l_1, l_2)^2$ . For a given  $J \in \mathbb{N}_0$ , we define  $h := (l_2 - l_1)/N_1$  with  $N_1 := 2^J$ . Recall the definition of  $(x_i, y_j)$  in (2.1). Let  $u(x, y)$  be the exact solution of (1.1) and  $(u_h)_{i,j}$  be the numerical solution at  $(x_i, y_j)$  using the mesh size  $h$ . We shall evaluate our proposed finite difference

scheme in the  $l_2$  norm by the relative error  $\frac{\|u_h - u\|_2}{\|u\|_2}$  if the exact solution  $u$  is available, and by the error  $\|u_h - u_{h/2}\|_2$  if the exact solution is not known, where

$$\|u_h - u\|_2^2 := h^2 \sum_{i=0}^{N_1} \sum_{j=0}^{N_1} ((u_h)_{i,j} - u(x_i, y_j))^2, \quad \|u_h - u_{h/2}\|_2^2 := h^2 \sum_{i=0}^{N_1} \sum_{j=0}^{N_1} ((u_h)_{i,j} - (u_{h/2})_{2i,2j})^2.$$

In the following numerical experiments, ‘[8]’, ‘[32]’ and ‘[35]’ correspond to the sixth order compact FDMs proposed in [8], [32] and [35] respectively. ‘Proposed’ corresponds to the sixth order compact FDM with reduced pollution effect in Section 2 of this paper. Recall that  $\frac{2\pi}{kh}$  corresponds to the number of points per wavelength.

**3.1. Numerical examples with no interfaces.** We provide four numerical experiments here.

**Example 3.1.** Consider the problem (1.1) in  $\Omega = (0, 1)^2$  with  $f = 0$  and all Dirichlet boundary conditions such that the boundary data  $g_1, \dots, g_4$  are picked such that the exact solution  $u(x, y, \theta) = \exp(ik(\cos(\theta)x + \sin(\theta)y))$  is the plane wave with the angle  $\theta$ . We define the following average error for plane wave solutions along all different angles  $\theta$  by

$$\frac{\|u_h - u\|_{2,w}}{\|u\|_{2,w}} := \frac{1}{N_3} \sum_{k=0}^{N_3-1} \sqrt{\frac{\sum_{i=0}^{N_1} \sum_{j=0}^{N_1} ((u_h)_{i,j,k} - u(x_i, y_j, \theta_k))^2}{\sum_{i=0}^{N_1} \sum_{j=0}^{N_1} (u(x_i, y_j, \theta_k))^2}},$$

where  $\theta_k = kh_\theta$ ,  $h_\theta = 2\pi/N_3$  for  $N_3 \in \mathbb{N}_0$ , and  $(u_h)_{i,j,k}$  is the value of the numerical solution  $u_h$  at the grid point  $(x_i, y_j)$  with a plane wave angle  $\theta_k$ . See Table 1 for numerical results.

TABLE 1. Numerical results for Example 3.1 with  $h = 1/2^J$ . The ratio  $r$  is equal to  $\frac{\|u_h - u\|_{2,w}}{\|u\|_{2,w}}$  of [8] divided by  $\frac{\|u_h - u\|_{2,w}}{\|u\|_{2,w}}$  of our proposed method. In other words, for the same mesh size  $h$  with  $h = 2^{-J}$ , the error of [8] is  $r$  times larger than that of our proposed method.

$J$	$k = 50, N_3 = 50$					$k = 150, N_3 = 30$					$k = 450, N_3 = 30$				
	[8]	Proposed		$\frac{2\pi}{kh}$	$r$	[8]	Proposed		$\frac{2\pi}{kh}$	$r$	[8]	Proposed		$\frac{2\pi}{kh}$	$r$
$\frac{\ u_h - u\ _{2,w}}{\ u\ _{2,w}}$	$\frac{\ u_h - u\ _{2,w}}{\ u\ _{2,w}}$	order	$\frac{\ u_h - u\ _{2,w}}{\ u\ _{2,w}}$			$\frac{\ u_h - u\ _{2,w}}{\ u\ _{2,w}}$	order	$\frac{\ u_h - u\ _{2,w}}{\ u\ _{2,w}}$			$\frac{\ u_h - u\ _{2,w}}{\ u\ _{2,w}}$	order	$\frac{\ u_h - u\ _{2,w}}{\ u\ _{2,w}}$		
4	9.83E+0	4.87E-01		2.0	<b>20.2</b>										
5	1.57E-02	1.01E-03	8.9	4.0	<b>15.5</b>										
6	5.01E-05	1.20E-05	6.4	8.0	<b>4.19</b>	3.67E+0	6.25E-02		2.7	<b>58.7</b>					
7	2.35E-07	1.77E-07	6.1	16.1	<b>1.33</b>	6.04E-03	6.82E-04	6.5	5.4	<b>8.85</b>					
8	2.78E-09	2.72E-09	6.0	32.2	<b>1.02</b>	2.56E-05	9.25E-06	6.2	10.7	<b>2.77</b>	1.26E+0	5.43E-02		3.6	<b>23.1</b>
9						1.78E-07	1.40E-07	6.0	21.4	<b>1.27</b>	4.72E-03	7.83E-04	6.1	7.1	<b>6.03</b>
10											2.25E-05	1.13E-05	6.1	14.3	<b>1.99</b>
11											1.85E-07	1.75E-07	6.0	28.6	<b>1.06</b>

**Example 3.2.** Consider the problem (1.1) in  $\Omega = (0, 1)^2$  with the boundary conditions

$$\begin{aligned} u(0, y) &= g_1, \quad \text{and} \quad u(1, y) = g_2 \quad \text{for} \quad y \in (0, 1), \\ u(x, 0) &= g_3, \quad \text{and} \quad u_y(x, 1) - iku(x, 1) = 0 \quad \text{for} \quad x \in (0, 1), \end{aligned}$$

where  $g_1, \dots, g_4$  and  $f$  are chosen such that the exact solution  $u = (y - 1) \cos(\alpha x) \sin(\beta(y - 1))$  with  $\alpha, \beta \in \mathbb{R}$ . See Tables 2 and 3 for numerical results for various choices of  $\alpha$  and  $\beta$ .

**Example 3.3.** Consider the problem (1.1) in  $\Omega = (0, 1)^2$  with boundary conditions in (2.20). I.e.,  $\mathcal{B}_1 u = \frac{\partial u}{\partial \bar{n}} - iku = g_1$  on  $\Gamma_1$ ,  $\mathcal{B}_2 u = u = g_2$  on  $\Gamma_2$ ,  $\mathcal{B}_3 u = \frac{\partial u}{\partial \bar{n}} = g_3$  on  $\Gamma_3$  and  $\mathcal{B}_4 u = \frac{\partial u}{\partial \bar{n}} - iku = g_4$  on  $\Gamma_4$ , where  $g_1, \dots, g_4$  and  $f$  are chosen such that the exact solution  $u = \sin(\alpha x + \beta y)$  with  $\alpha, \beta \in \mathbb{R}$ . See Table 4 for numerical results for various choices of  $\alpha$  and  $\beta$ .

TABLE 2. Numerical results of Example 3.2 with  $h = 1/2^J$  and  $k = 300$ . The ratio  $r_1$  is equal to  $\frac{\|u_h - u\|_2}{\|u\|_2}$  of [32] divided by  $\frac{\|u_h - u\|_2}{\|u\|_2}$  of our proposed method and the ratio  $r_2$  is equal to  $\frac{\|u_h - u\|_2}{\|u\|_2}$  of [35] divided by  $\frac{\|u_h - u\|_2}{\|u\|_2}$  of our proposed method. In other words, for the same grid size  $h$  with  $h = 2^{-J}$ , the errors of [32] and [35] are  $r_1$  and  $r_2$  times larger than those of our proposed method, respectively.

		$\alpha = 50, \beta = 290$					$\alpha = 100, \beta = 275$					$\alpha = 150, \beta = 255$				
		[32]	[35]	Proposed		[32]	[35]	Proposed		[32]	[35]	Proposed				
$J$	$\frac{2\pi}{kh}$	$\frac{\ u_h - u\ _2}{\ u\ _2}$	$\frac{\ u_h - u\ _2}{\ u\ _2}$	$\frac{\ u_h - u\ _2}{\ u\ _2}$	$r_1$	$r_2$	$\frac{\ u_h - u\ _2}{\ u\ _2}$	$\frac{\ u_h - u\ _2}{\ u\ _2}$	$\frac{\ u_h - u\ _2}{\ u\ _2}$	$r_1$	$r_2$	$\frac{\ u_h - u\ _2}{\ u\ _2}$	$\frac{\ u_h - u\ _2}{\ u\ _2}$	$\frac{\ u_h - u\ _2}{\ u\ _2}$	$r_1$	$r_2$
7	2.7	1.1E+0	9.8E-02	3.8E-02	<b>29</b>	<b>2.6</b>	2.4E+0	2.1E-01	4.4E-02	<b>54</b>	<b>4.6</b>	4.4E+0	1.2E-01	5.8E-02	<b>77</b>	<b>2.1</b>
8	5.4	8.6E-03	6.1E-04	1.3E-04	<b>65</b>	<b>4.6</b>	1.2E-02	1.3E-03	3.1E-04	<b>40</b>	<b>4.4</b>	1.7E-02	8.3E-04	1.3E-04	<b>134</b>	<b>6.5</b>
9	10.7	1.2E-04	8.4E-06	2.8E-06	<b>43</b>	<b>3.0</b>	1.7E-04	1.8E-05	5.7E-06	<b>30</b>	<b>3.2</b>	2.4E-04	1.1E-05	2.0E-06	<b>121</b>	<b>5.7</b>
10	21.4	1.8E-06	1.2E-07	4.6E-08	<b>39</b>	<b>2.6</b>	2.6E-06	2.7E-07	9.2E-08	<b>28</b>	<b>2.9</b>	3.7E-06	1.7E-07	3.3E-08	<b>114</b>	<b>5.1</b>

TABLE 3. Numerical results of Example 3.2 with  $h = 1/2^J$  and  $k = 300$ . The ratio  $r_1$  is equal to  $\frac{\|u_h - u\|_2}{\|u\|_2}$  of [32] divided by  $\frac{\|u_h - u\|_2}{\|u\|_2}$  of our proposed method and the ratio  $r_2$  is equal to  $\frac{\|u_h - u\|_2}{\|u\|_2}$  of [35] divided by  $\frac{\|u_h - u\|_2}{\|u\|_2}$  of our proposed method. In other words, for the same grid size  $h$  with  $h = 2^{-J}$ , the errors of [32] and [35] are  $r_1$  and  $r_2$  times larger than those of our proposed method, respectively.

		$\alpha = 200, \beta = 200$					$\alpha = 250, \beta = 160$					$\alpha = 290, \beta = 50$				
		[32]	[35]	Proposed		[32]	[35]	Proposed		[32]	[35]	Proposed				
$J$	$\frac{2\pi}{kh}$	$\frac{\ u_h - u\ _2}{\ u\ _2}$	$\frac{\ u_h - u\ _2}{\ u\ _2}$	$\frac{\ u_h - u\ _2}{\ u\ _2}$	$r_1$	$r_2$	$\frac{\ u_h - u\ _2}{\ u\ _2}$	$\frac{\ u_h - u\ _2}{\ u\ _2}$	$\frac{\ u_h - u\ _2}{\ u\ _2}$	$r_1$	$r_2$	$\frac{\ u_h - u\ _2}{\ u\ _2}$	$\frac{\ u_h - u\ _2}{\ u\ _2}$	$\frac{\ u_h - u\ _2}{\ u\ _2}$	$r_1$	$r_2$
7	2.7	1.1E+0	1.3E-01	1.4E-01	<b>8</b>	<b>0.9</b>	6.0E+0	1.8E-01	4.8E-02	<b>125</b>	<b>3.7</b>	8.9E+0	1.3E-01	5.5E-02	<b>162</b>	<b>2.4</b>
8	5.4	7.5E-03	9.7E-04	3.8E-04	<b>20</b>	<b>2.6</b>	4.0E-02	1.1E-03	8.1E-05	<b>492</b>	<b>14.1</b>	9.8E-03	7.4E-04	1.5E-04	<b>66</b>	<b>4.9</b>
9	10.7	1.1E-04	1.3E-05	3.4E-06	<b>33</b>	<b>3.9</b>	5.6E-04	1.6E-05	2.1E-06	<b>264</b>	<b>7.6</b>	1.5E-04	1.0E-05	1.6E-06	<b>92</b>	<b>6.2</b>
10	21.4	1.7E-06	2.0E-07	4.5E-08	<b>38</b>	<b>4.4</b>	8.6E-06	2.3E-07	3.7E-08	<b>234</b>	<b>6.3</b>	2.3E-06	1.5E-07	2.3E-08	<b>101</b>	<b>6.4</b>

TABLE 4. Numerical results of Example 3.3 with  $h = 1/2^J$  using our proposed method.

		$k = 450, \alpha = 400, \beta = 200$					$k = 600, \alpha = 300, \beta = 500$				
$J$	$\frac{2\pi}{kh}$	$\frac{\ u_h - u\ _2}{\ u\ _2}$	order	$\ u_h - u_{h/2}\ _2$	order	$\frac{2\pi}{kh}$	$\frac{\ u_h - u\ _2}{\ u\ _2}$	order	$\ u_h - u_{h/2}\ _2$	order	
7	1.79	1.3753E+01		9.8073E+00		1.34	9.0200E+01		6.4272E+01		
8	3.57	1.7358E-02	9.630	1.2212E-02	9.649	2.68	9.4259E-02	9.902	6.6801E-02	9.910	
9	7.15	1.6528E-04	6.715	1.1540E-04	6.725	5.36	2.7428E-04	8.425	1.9430E-04	8.425	
10	14.30	2.4370E-06	6.084	1.6971E-06	6.087	10.72	1.7971E-06	7.254	1.2453E-06	7.286	
11	28.60	3.9410E-08	5.950			21.45	4.5869E-08	5.292			

**Example 3.4.** Consider the problem (1.1) in  $\Omega = (0, 1)^2$  with boundary conditions in (2.20), where  $f(x, y) = k^2 \sin(8x) \cos(6y)$ ,  $g_1 = \sin(5y)$ ,  $g_2 = 0$ ,  $g_3 = (x - 1) \sin(4x)$ , and  $g_4 = \cos(5x)$ . Note that the exact solution  $u$  is unknown in this example. See Table 5 and Fig. 2 for numerical results.

TABLE 5. Numerical results of Example 3.4 with  $h = 1/2^J$  using our proposed method.

		$k = 200$				$k = 400$				$k = 800$			
$J$	$\frac{2\pi}{kh}$	$\ u_h - u_{h/2}\ _2$	order	$\ u_h\ _2$	$\frac{2\pi}{kh}$	$\ u_h - u_{h/2}\ _2$	order	$\ u_h\ _2$	$\frac{2\pi}{kh}$	$\ u_h - u_{h/2}\ _2$	order	$\ u_h\ _2$	
6	2.01	8.776E-01		5.81E-01									
7	4.02	3.716E-03	7.88	9.84E-01	2.01	7.936E-01		5.28E-01					
8	8.04	4.430E-05	6.39	9.81E-01	4.02	7.410E-03	6.74	9.76E-01	2.01	8.453E-01		5.08E-01	
9	16.08			9.80E-01	8.04	8.579E-05	6.43	9.75E-01	4.02	1.486E-02	5.83	9.70E-01	
10					16.08			9.74E-01	8.04	1.715E-04	6.44	9.70E-01	
11									16.08			9.69E-01	

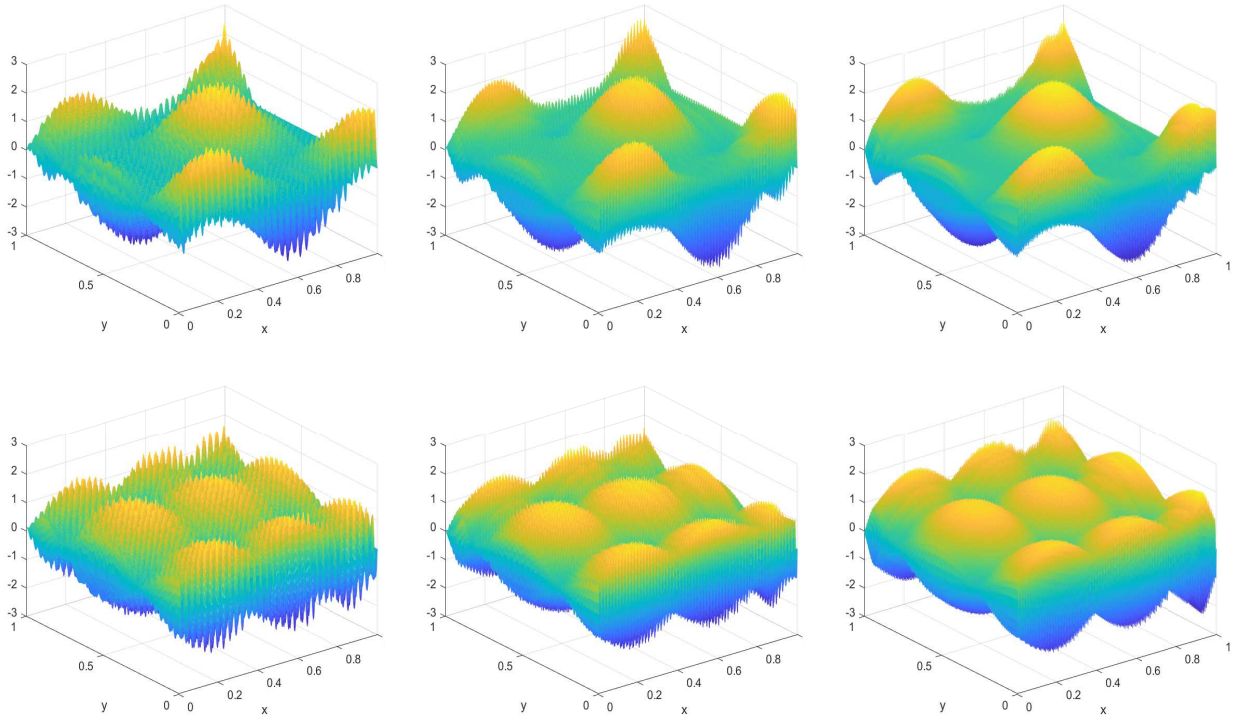


FIGURE 2. First row: the real part of  $u_h$  in Example 3.4, where  $k = 200$  and  $h = 1/2^9$  (left),  $k = 400$  and  $h = 1/2^{10}$  (middle),  $k = 800$  and  $h = 1/2^{11}$  (right). Second row: the imaginary part of  $u_h$  in Example 3.4, where  $k = 200$  and  $h = 1/2^9$  (left),  $k = 400$  and  $h = 1/2^{10}$  (middle),  $k = 800$  and  $h = 1/2^{11}$  (right).

**3.2. Numerical examples with interfaces.** We provide three numerical experiments here.

**Example 3.5.** Consider the problem (1.1) in  $\Omega = (-3/2, 3/2)^2$  with boundary conditions in (2.20), where  $k = 100$ ,  $\Gamma_I := \{(x, y) \in \Omega : \psi(x, y) = 0\}$  with  $\psi(x, y) = y^2/2 + x^2/(1+x^2) - 1/2$  (see Fig. 3 (left)),  $g_D = -1$ , and  $g_N = 0$ . The boundary data  $g_1, \dots, g_4$  and  $f_{\pm}$  are chosen such that the exact solution  $u$  is given by  $u_+ = u\chi_{\Omega^+} = \cos(50x)\cos(80y)$  and  $u_- = u\chi_{\Omega^-} = \cos(50x)\cos(80y) + 1$ . See Table 6 for numerical results.

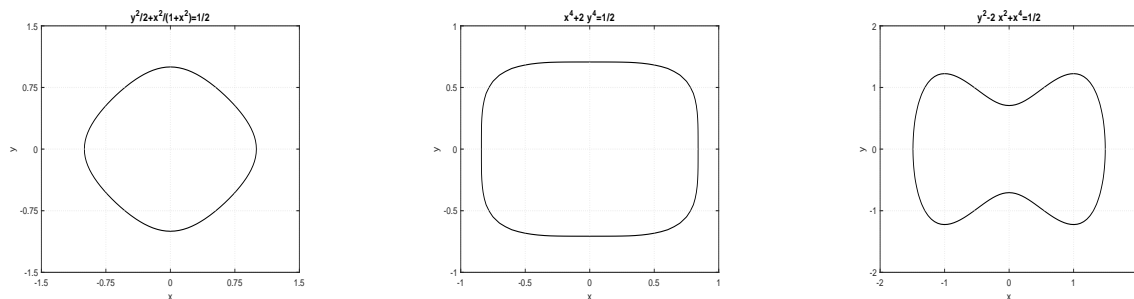


FIGURE 3.  $y^2/2 + x^2/(1+x^2) = 1/2$  (left),  $x^4 + 2y^4 = 1/2$  (middle), and  $y^2 - 2x^2 + x^4 = 1/2$  (right).

**Example 3.6.** Consider the problem (1.1) in  $\Omega = (-1, 1)^2$  with boundary conditions in (2.20), where  $k = 300$ ,  $\Gamma_I := \{(x, y) \in \Omega : \psi(x, y) = 0\}$  with  $\psi(x, y) = x^4 + 2y^4 - 1/2$  (see Fig. 3 (middle)),  $f_+ = 75^2 \sin(3(x+y))$ ,  $f_- = 75^2 \cos(4x)\cos(3y)$ ,  $g_D = \sin(2\pi x)\sin(2\pi y) + 3$ , and  $g_N = \cos(2\pi x)\cos(2\pi y)$ . The following boundary data are given by  $g_1 = e^y + e^{-y}$ ,  $g_2 = 0$ ,  $g_3 = (x-1)e^x$ , and  $g_4 = \sin(2x)$ . Note that the exact solution  $u$  is unknown in this example. See Table 6 for numerical results.

**Example 3.7.** Consider the problem (1.1) in  $\Omega = (-2, 2)^2$  with boundary conditions in (2.20), where  $k = 150$ ,  $\Gamma_I := \{(x, y) \in \Omega : \psi(x, y) = 0\}$  with  $\psi(x, y) = y^2 - 2x^2 + x^4 - 1/2$  (see Fig. 3 (right)),

$f_+ = \sin(5(x - y))$ ,  $f_- = 10^4 \sin(5x) \sin(5y)$ ,  $g_D = \sin(2\pi(x - y))$ , and  $g_N = \cos(2\pi(x + y))$ . The following boundary data are given by  $g_1 = \cos(y) \sin(y)$ ,  $g_2 = 0$ ,  $g_3 = \sin(2x - 4)$ , and  $g_4 = e^x \sin(x)$ . Note that the exact solution  $u$  is unknown in this example. See Table 6 for numerical results.

TABLE 6. Numerical results of Examples 3.5 to 3.7 with  $h = (l_2 - l_1)/2^J$  using our proposed method.

$J$	Example 3.5 with $h = \frac{3}{2^J}$				Example 3.6 with $h = \frac{2}{2^J}$				Example 3.7 with $h = \frac{4}{2^J}$				
	$\frac{2\pi}{hk}$	$\frac{\ u_h - u\ _2}{\ u\ _2}$	order	$\ u_h - u_{h/2}\ _2$	order	$\frac{2\pi}{hk}$	$\ u_h - u_{h/2}\ _2$	order	$\ u_{h/2}\ _2$	$\frac{2\pi}{hk}$	$\ u_h - u_{h/2}\ _2$	order	$\ u_{h/2}\ _2$
7	2.7	1.28E+00		2.90E+00									
8	5.4	2.44E-03	9.0	5.51E-03	9.0	2.7	1.06E+01		7.039	2.7	8.19E+00		3.467
9	10.7	5.82E-06	8.7	1.31E-05	8.7	5.4	1.49E-02	9.5	7.037	5.4	7.96E-03	10.0	3.469
10	21.4	3.98E-08	7.2	9.27E-08	7.1	10.7	1.69E-04	6.5	7.035	10.7	7.66E-05	6.7	3.468

#### 4. PROOFS OF THEOREMS 2.2 TO 2.5

In this section, we prove the main results stated in Section 2. The idea of proofs is to first construct all possible compact stencils with the maximum accuracy order and then to minimize the average truncation error of plane waves over the free parameters of stencils to reduce pollution effect.

*Proof of Theorem 2.2.* We first find all stencil coefficients  $\{C_{k,\ell}\}_{k,\ell \in \{-1,0,1\}}$  and  $\{C_{f,m,n}\}_{(m,n) \in \Lambda_{M_f-1}}$  such that

$$\sum_{k=-1}^1 \sum_{\ell=-1}^1 C_{k,\ell} u(x_i + kh, y_j + \ell h) = \sum_{(m,n) \in \Lambda_{M_f-1}} f^{(m,n)} C_{f,m,n} + \mathcal{O}(h^{M+2}), \quad h \rightarrow 0,$$

for some  $M, M_f \in \mathbb{N}_0$  and  $M_f \geq M$ . Afterwards, we set the remaining free parameters by minimizing the average truncation error of plane waves. Approximating  $u(x_i + kh, y_j + \ell h)$  as in (2.12), we have

$$\sum_{(m,n) \in \Lambda_{M+1}^{V,1}} u^{(m,n)} I_{m,n} + \sum_{(m,n) \in \Lambda_{M_f-1}} f^{(m,n)} (J_{m,n} - C_{f,m,n}) = \mathcal{O}(h^{M+2}), \quad h \rightarrow 0, \quad (4.1)$$

where we define

$$I_{m,n} := \sum_{k=-1}^1 \sum_{\ell=-1}^1 C_{k,\ell} G_{M,m,n}^V(kh, \ell h), \quad \text{and} \quad J_{m,n} := \sum_{k=-1}^1 \sum_{\ell=-1}^1 C_{k,\ell} Q_{M_f,m,n}^V(kh, \ell h). \quad (4.2)$$

Solving (4.1) is equivalent to solving

$$I_{m,n} = \mathcal{O}(h^{M+2}), \quad h \rightarrow 0, \quad \text{for all } (m,n) \in \Lambda_{M+1}^{V,1}, \quad (4.3)$$

$$C_{f,m,n} = J_{m,n} + \mathcal{O}(h^{M+2}), \quad h \rightarrow 0, \quad \text{for all } (m,n) \in \Lambda_{M_f-1}. \quad (4.4)$$

We set  $C_{k,\ell} := \sum_{j=0}^{M+1} c_{k,\ell,j} (kh)^j$ , where  $c_{k,\ell,j} \in \mathbb{R}$  for all  $k, \ell \in \{-1,0,1\}$ . Furthermore, we let  $C_{-1,-1} = C_{-1,1} = C_{1,-1} = C_{1,1}$  and  $C_{-1,0} = C_{0,-1} = C_{0,1} = C_{1,0}$  for symmetry. By calculation, we find that  $M = 6$  is the maximum positive integer such that the linear system (4.3) has a non-trivial solution. All such non-trivial solutions for  $M = 6$  can be uniquely written (up to a constant multiple) as

$$\begin{aligned} C_{1,1} &= c_9(kh)^7 + c_3(kh)^6 + c_2(kh)^5 + c_1(kh)^4 + (-12c_2 + c_4 - 6c_6 + 24c_{10} + 6c_{11} + 24c_9)(kh)^3 + (1/15 + 4c_1 + 2c_5 - 8c_7 - 2c_8 \\ &\quad - 8c_3)(kh)^2 + (-240c_2 + 15c_4 - 120c_6 + 480c_{10} + 120c_{11} + 480c_9)(kh) + 1 \\ C_{1,0} &= c_{10}(kh)^7 + c_7(kh)^6 + c_6(kh)^5 + c_5(kh)^4 + c_4(kh)^3 + (1/15 + 16c_1 + 8c_5 - 32c_7 - 8c_8 - 32c_3)(kh)^2 + (-960c_2 + 60c_4 \\ &\quad - 480c_6 + 1920c_{10} + 480c_{11} + 1920c_9)(kh) + 4 \\ C_{0,0} &= c_{11}(kh)^7 + c_8(kh)^6 + (92c_2 - (9/2)c_4 + 44c_6 - 192c_{10} - 48c_{11} - 192c_9)(kh)^5 + (-3/10 + 20c_1 + 8c_5 - 48c_7 - 12c_8 \\ &\quad - 48c_3)(kh)^4 + (-1392c_2 + 82c_4 - 696c_6 + 2784c_{10} + 696c_{11} + 2784c_9)(kh)^3 + (82/15 - 80c_1 - 40c_5 + 160c_7 + 40c_8 \\ &\quad + 160c_3)(kh)^2 + (4800c_2 - 300c_4 + 2400c_6 - 9600c_{10} - 2400c_{11} - 9600c_9)(kh) - 20, \end{aligned} \quad (4.5)$$

where  $c_i \in \mathbb{R}$  for  $i = 1, \dots, 11$  are free parameters. Note that any interior symmetric compact stencil has accuracy order 6 if and only if the 7th-degree Taylor polynomials of the stencil coefficients are given by (4.5). Choosing  $M_f = 7$  in (4.2) and (4.4) yields the right-hand side of (2.15).

Next, consider a general compact stencil  $\{C_{k,\ell}^w\}_{k,\ell \in \{-1,0,1\}}$  parameterized by  $C_{1,1}^w, C_{1,0}^w \in \mathbb{R}$  satisfying

$$C_{-1,-1}^w = C_{-1,1}^w = C_{1,-1}^w = C_{1,1}^w, \quad C_{-1,0}^w = C_{0,-1}^w = C_{0,1}^w = C_{1,0}^w, \quad \text{and} \quad C_{0,0}^w = -20,$$

where we normalized the stencil by  $C_{0,0}^w = -20$ . Take a plane wave solution  $u(x, y, \theta) := \exp(\mathbf{i}k(\cos(\theta)x + \sin(\theta)y))$  for any  $\theta \in [0, 2\pi)$ . Clearly, we have  $\Delta u + \mathbf{k}^2 u = 0$ . Hence, the truncation error associated with the general compact stencil coefficients  $\{C_{k,\ell}^w\}_{k,\ell \in \{-1,0,1\}}$  at the grid point  $(x_i, y_j) \notin \partial\Omega$  is

$$(T(\theta|kh))_{x_i, y_j} := \sum_{k=-1}^1 \sum_{\ell=-1}^1 C_{k,\ell}^w \exp(\mathbf{i}k(\cos(\theta)(x_i + kh) + \sin(\theta)(y_j + \ell h))).$$

Recall that  $\frac{2\pi}{kh}$  is the number of points per wavelength. Hence, it is reasonable to choose  $kh \in [1/4, 1]$ . Without loss of generality, we let  $(x_i, y_j) = (0, 0)$ . Define  $S := \{\frac{1}{4} + \frac{3s}{4000} : s = 0, \dots, 1000\}$  and let

$$(\tilde{C}_{1,1}^w(kh), \tilde{C}_{1,0}^w(kh)) := \arg \min_{C_{1,1}^w, C_{1,0}^w \in \mathbb{R}} \int_0^{2\pi} |(T(\theta|kh))_{0,0}|^2 d\theta, \quad kh \in S. \quad (4.6)$$

We use the Simpson's 3/8 rule with 900 uniform sampling points to calculate  $\int_0^{2\pi} |(T(\theta|kh))_{0,0}|^2 d\theta$ . Now, we link  $C_{0,0}, C_{1,0}, C_{1,1}$  in (4.5) with  $C_{0,0}^w, \tilde{C}_{1,0}^w(kh), \tilde{C}_{1,1}^w(kh)$  in (4.6) for  $kh \in S$ . To further simplify the presentation of our stencil coefficients, we set  $c_9 = c_{10} = c_{11} = 0$  in (4.5) so that the coefficients of the polynomials in (4.5) for degree 7 are zero. Because  $C_{0,0}^w = -20$  is our normalization, we determine the free parameters  $c_i$  for  $i = 1, \dots, 8$  in (4.5) by considering the following least-square problem:

$$(\tilde{c}_1, \tilde{c}_2, \dots, \tilde{c}_8) := \arg \min_{c_1, c_2, \dots, c_8 \in \mathbb{R}} \sum_{kh \in S} |C_{1,1}(kh) - \tilde{C}_{1,1}^w(kh)C_{0,0}(kh)/(-20)|^2 + |C_{1,0}(kh) - \tilde{C}_{1,0}^w(kh)C_{0,0}(kh)/(-20)|^2.$$

For simplicity of presentation, we replace each above calculated coefficient  $\tilde{c}_i$  with its approximated fractional form  $[10^8 \tilde{c}_i]/10^8$ , where  $[\cdot]$  is a rounding operation to the nearest integer. Plugging these approximated fractional forms into coefficients  $c_i$  for  $i = 1, \dots, 8$  in (4.5), we obtain (2.16).  $\square$

*Proof of Theorem 2.3.* We only prove item (1). The proof of item (2) is very similar. We start by finding all stencil coefficients  $\{C_{k,\ell}^{\mathcal{B}_1}\}_{k,\ell \in \{0,1\}, \ell \in \{-1,0,1\}}$ ,  $\{C_{f,m,n}^{\mathcal{B}_1}\}_{(m,n) \in \Lambda_{M_f-1}}$  and  $\{C_{g_1,n}^{\mathcal{B}_1}\}_{n=0}^{M_{g_1}}$  such that

$$\sum_{k=0}^1 \sum_{\ell=-1}^1 C_{k,\ell}^{\mathcal{B}_1} u(x_i + kh, y_j + \ell h) = \sum_{(m,n) \in \Lambda_{M_f-1}} f^{(m,n)} C_{f,m,n}^{\mathcal{B}_1} + \sum_{n=0}^{M_{g_1}} g_1^{(n)} C_{g_1,n}^{\mathcal{B}_1} + \mathcal{O}(h^{M+2}), \quad h \rightarrow 0 \quad (4.7)$$

for some  $M_f, M_{g_1}, M \in \mathbb{N}_0$ ,  $M_f \geq M$  and  $M_{g_1} \geq M$ . Afterwards, we set the remaining free parameters by minimizing the average truncation error of plane waves.

Since  $-u_x - \mathbf{i}ku = g_1$  on  $\Gamma_1$ , we have  $u^{(1,n)} = -\mathbf{i}ku^{(0,n)} - g_1^{(n)}$  for all  $n = 0, \dots, M_{g_1}$ . By (2.12),

$$\begin{aligned} u(x + x_i^*, y + y_j^*) &= \sum_{n=0}^{M+1} u^{(0,n)} G_{M,0,n}^V(x, y) + \sum_{n=0}^M u^{(1,n)} G_{M,1,n}^V(x, y) + \sum_{(m,n) \in \Lambda_{M_f-1}} f^{(m,n)} Q_{M_f,m,n}^V(x, y) + \mathcal{O}(h^{M+2}) \\ &= \sum_{n=0}^{M+1} u^{(0,n)} G_{M,0,n}^V(x, y) + \sum_{n=0}^{M_{g_1}} u^{(1,n)} G_{M_{g_1},1,n}^V(x, y) + \sum_{(m,n) \in \Lambda_{M_f-1}} f^{(m,n)} Q_{M_f,m,n}^V(x, y) + \mathcal{O}(h^{M+2}) \\ &= \sum_{n=0}^{M+1} u^{(0,n)} G_{M,0,n}^V(x, y) - \sum_{n=0}^{M_{g_1}} (\mathbf{i}ku^{(0,n)} + g_1^{(n)}) G_{M_{g_1},1,n}^V(x, y) + \sum_{(m,n) \in \Lambda_{M_f-1}} f^{(m,n)} Q_{M_f,m,n}^V(x, y) + \mathcal{O}(h^{M+2}) \\ &= u^{(0,M+1)} G_{M,0,M+1}^V(x, y) + \sum_{n=0}^M u^{(0,n)} \left( G_{M,0,n}^V(x, y) - \mathbf{i}k G_{M,1,n}^V(x, y) \right) - \sum_{n=0}^{M_{g_1}} g_1^{(n)} G_{M_{g_1},1,n}^V(x, y) \end{aligned}$$



$$+ \sum_{(m,n) \in \Lambda_{M_f-1}} f^{(m,n)} Q_{M_f,m,n}^V(x,y) + \mathcal{O}(h^{M+2}), \quad \text{for } x, y \in (-2h, 2h).$$

Approximating  $u(x_i + kh, y_j + \ell h)$  in (4.7), we have

$$\sum_{n=0}^{M+1} u^{(0,n)} I_n^{\mathcal{B}_1} + \sum_{(m,n) \in \Lambda_{M_f-1}} f^{(m,n)} (J_{m,n}^{\mathcal{B}_1} - C_{f,m,n}^{\mathcal{B}_1}) + \sum_{n=0}^{M_{g_1}} g_1^{(n)} (K_n^{\mathcal{B}_1} - C_{g_1,n}^{\mathcal{B}_1}) = \mathcal{O}(h^{M+2}), \quad (4.8)$$

as  $h \rightarrow 0$ , where

$$I_n^{\mathcal{B}_1} := \sum_{k=0}^1 \sum_{\ell=-1}^1 C_{k,\ell}^{\mathcal{B}_1} (G_{M,0,n}^V(kh, \ell h) - ik G_{M,1,n}^V(kh, \ell h)(1 - \delta_{n,M+1})),$$

$$J_{m,n}^{\mathcal{B}_1} := \sum_{k=0}^1 \sum_{\ell=-1}^1 C_{k,\ell}^{\mathcal{B}_1} Q_{M_f,m,n}^V(kh, \ell h), \quad K_n^{\mathcal{B}_1} := - \sum_{k=0}^1 \sum_{\ell=-1}^1 C_{k,\ell}^{\mathcal{B}_1} G_{M_{g_1},1,n}^V(kh, \ell h), \quad (4.9)$$

$\delta_{a,a} = 1$ , and  $\delta_{a,b} = 0$  for  $a \neq b$ . We set  $C_{k,\ell}^{\mathcal{B}_1} := \sum_{j=0}^{M+1} (c_{k,\ell,j} + id_{k,\ell,j})(kh)^j$ , where  $c_{k,\ell,j}, d_{k,\ell,j} \in \mathbb{R}$  for all  $k \in \{0, 1\}$  and  $\ell \in \{-1, 0, 1\}$ . Furthermore, we let  $C_{0,-1}^{\mathcal{B}_1} = C_{0,1}^{\mathcal{B}_1}$  and  $C_{1,-1}^{\mathcal{B}_1} = C_{1,1}^{\mathcal{B}_1}$  for symmetry. By calculation, we find that  $M = 5$  is the maximum positive integer such that the linear system of (4.8) has a non-trivial solution. To further simplify such a solution, we set coefficients associated with  $kh$  of degrees higher than 4 to zero; i.e., we now have polynomials of  $kh$ , whose highest degree is now 4. All such non-trivial solutions for  $M = 5$  can be uniquely written (up to a constant multiple) as

$$\begin{aligned} C_{1,1}^{\mathcal{B}_1} &= (c_3 + ic_7)(kh)^4 + (c_2 + ic_6)(kh)^3 + 12(ic_8 - (7i/3)c_2 + (7i/3)c_5 + (13i/3)c_7 + (7/3)c_1 + (13/3)c_3 + c_4 + (7/3)c_6 - 4/135)(kh)^2 \\ &\quad - 60(ic_1 + 2ic_3 + (i/2)c_4 + ic_6 - 4i/225 - (1/2)c_8 + c_2 - c_5 - 2c_7)kh + 1 \\ C_{0,1}^{\mathcal{B}_1} &= (c_1 + ic_5)(kh)^4 + 13(ic_1 + (20i/13)c_3 + (7i/26)c_4 + (12i/13)c_6 - 17i/1170 - (7/26)c_8 + (12/13)c_2 - c_5 - (20/13)c_7)(kh)^3 \\ &\quad + 18(ic_8 - (22i/9)c_2 + (22i/9)c_5 + (40i/9)c_7 + (22/9)c_1 + (40/9)c_3 + c_4 + (22/9)c_6 - 11/324)(kh)^2 - 120(ic_1 + (2i)c_3 + (i/2)c_4 \\ &\quad + ic_6 - 29i/1800 - (1/2)c_8 + c_2 - c_5 - 2c_7)kh + 2 \\ C_{1,0}^{\mathcal{B}_1} &= (c_4 + ic_8)(kh)^4 + 18(ic_1 + (4i/3)c_3 + (i/6)c_4 + (8i/9)c_6 - i/90 - (1/6)c_8 + (8/9)c_2 - c_5 - (4/3)c_7)(kh)^3 + 36(ic_8 - (22i/9)c_2 \\ &\quad + (22i/9)c_5 + (40i/9)c_7 + (22/9)c_1 + (40/9)c_3 + c_4 + (22/9)c_6 - 49/1620)(kh)^2 - 240(ic_1 + (2i)c_3 + (i/2)c_4 + ic_6 - 29i/1800 \\ &\quad - (1/2)c_8 + c_2 - c_5 - 2c_7)kh + 4 \\ C_{0,0}^{\mathcal{B}_1} &= -4(ic_8 - (3i/2)c_2 + (2i)c_5 + (7i/2)c_7 + 2c_1 + (7/2)c_3 + c_4 + (3/2)c_6 - 1/80)(kh)^4 - 80(ic_1 + (2i)c_3 + (i/2)c_4 + (39i/40)c_6 \\ &\quad - 7i/720 - (1/2)c_8 + (39/40)c_2 - c_5 - 2c_7)(kh)^3 + 84(ic_8 - (32i/21)c_2 + (32i/21)c_5 + (74i/21)c_7 + (32/21)c_1 + (74/21)c_3 + c_4 \\ &\quad + (32/21)c_6 + 1/3780)(kh)^2 + 600(ic_1 + (2i)c_3 + (i/2)c_4 + ic_6 - 29i/4500 - (1/2)c_8 + c_2 - c_5 - 2c_7)kh - 10, \end{aligned} \quad (4.10)$$

where each  $c_i \in \mathbb{R}$  for  $i = 1, \dots, 8$  are free parameters. Choosing  $M_f = M_{g_1} = 7$  in (4.8) and (4.9) yields the right-hand side of (2.17).

Next, consider a compact stencil  $\{C_{k,\ell}^w\}_{k \in \{0,1\}, \ell \in \{-1,0,1\}}$  parameterized by  $C_{1,1}^w, C_{0,1}^w, C_{1,0}^w \in \mathbb{C}$  with

$$C_{1,-1}^w = C_{1,1}^w, \quad C_{0,-1}^w = C_{0,1}^w, \quad \text{and} \quad C_{0,0}^w = -10,$$

where we normalized the general stencil by  $C_{0,0}^w = -10$ . Take a plane wave solution  $u(x, y, \theta) := \exp(ik(\cos(\theta)x + \sin(\theta)y))$  for any  $\theta \in [0, 2\pi)$ . Clearly, we have  $\Delta u + k^2 u = 0$  and  $-u_x - iku = g_1 \neq 0$  on  $\Gamma_1$ , where  $g_1$  and its derivatives are explicitly known by plugging the plane wave solution  $u(x, y, \theta)$  into the boundary condition. Hence, the truncation error associated with the compact general stencil coefficients  $\{C_{k,\ell}^w\}_{k \in \{0,1\}, \ell \in \{-1,0,1\}}$  at the grid point  $(x_0, y_j) \in \Gamma_1$  is

$$(T(\theta|kh))_{x_0, y_j} := \sum_{k=0}^1 \sum_{\ell=-1}^1 C_{k,\ell}^w \exp(ik(\cos(\theta)(x_0 + kh) + \sin(\theta)(y_j + \ell h))) + \sum_{n=0}^7 g_1^{(n)} \sum_{k=0}^1 \sum_{\ell=-1}^1 C_{k,\ell}^w G_{7,1,n}^V(kh, \ell h).$$

Without loss of generality, we let  $(x_0, y_j) = (0, 0)$ . Afterwards, we follow a similar minimization procedure as in the proof of Theorem 2.2 to obtain the concrete stencils in Theorem 2.3.  $\square$

*Proof of Theorem 2.4.* We start by finding all stencil coefficients  $\{C_{k,\ell}^{\mathcal{R}_1}\}_{k,\ell \in \{0,1\}}$ ,  $\{C_{f,m,n}^{\mathcal{R}_1}\}_{(m,n) \in \Lambda_{M_f-1}}$ ,  $\{C_{g_1,n}^{\mathcal{R}_1}\}_{n=0}^{M_{g_1}}$ , and  $\{C_{g_3,n}^{\mathcal{R}_1}\}_{n=0}^{M_{g_3}}$  such that

$$\sum_{k=0}^1 \sum_{\ell=0}^1 C_{k,\ell}^{\mathcal{R}_1} u(x_0 + kh, y_0 + \ell h) = \sum_{(m,n) \in \Lambda_{M_f-1}} f^{(m,n)} C_{f,m,n}^{\mathcal{R}_1} + \sum_{n=0}^{M_{g_1}} g_1^{(n)} C_{g_1,n}^{\mathcal{R}_1} + \sum_{n=0}^{M_{g_3}} g_3^{(n)} C_{g_3,n}^{\mathcal{R}_1} + \mathcal{O}(h^{M+2}), \quad (4.11)$$

$h \rightarrow 0$ , for some  $M, M_f, M_{g_1}, M_{g_3} \in \mathbb{N}_0$ ,  $M_f \geq M$ ,  $M_{g_1} \geq M$  and  $M_{g_3} \geq M$ . Afterwards, we set the remaining free parameters by minimizing the average truncation error of plane waves.

Note that we have

$$u^{(1,n)} = -iku^{(0,n)} - g_1^{(n)} \quad \text{and} \quad u^{(m,1)} = -g_3^{(m)}, \quad \text{for all } m, n \in \mathbb{N}_0. \quad (4.12)$$

Let  $C_{k,\ell}^{\mathcal{R}_1} := C_{k,\ell}^{\mathcal{R}_1,V} + C_{k,\ell}^{\mathcal{R}_1,H}$  for  $k, \ell \in \{0, 1\}$ , where  $C_{k,\ell}^{\mathcal{R}_1,V}$  and  $C_{k,\ell}^{\mathcal{R}_1,H}$  are to be determined polynomials of  $h$ . Approximating  $u(x_0 + kh, y_0 + \ell h)$  with (2.12), (2.13), and using (4.12), we have

$$\begin{aligned} \sum_{k=0}^1 \sum_{\ell=0}^1 (C_{k,\ell}^{\mathcal{R}_1,V} + C_{k,\ell}^{\mathcal{R}_1,H}) u(x_0 + kh, y_0 + \ell h) &= \sum_{n=0}^{M+1} u^{(0,n)} I_n^{\mathcal{R}_1,V} + \sum_{m=0}^{M+1} u^{(m,0)} I_m^{\mathcal{R}_1,H} \\ &+ \sum_{(m,n) \in \Lambda_{M_f-1}} f^{(m,n)} J_{m,n}^{\mathcal{R}_1} + \sum_{n=0}^{M_{g_1}} g_1^{(n)} K_n^{\mathcal{R}_1,V} + \sum_{m=0}^{M_{g_3}} g_3^{(m)} K_m^{\mathcal{R}_1,H} + \mathcal{O}(h^{M+2}), \end{aligned} \quad (4.13)$$

where

$$\begin{aligned} I_n^{\mathcal{R}_1,V} &:= \sum_{k=0}^1 \sum_{\ell=0}^1 C_{k,\ell}^{\mathcal{R}_1,V} (G_{M,0,n}^V(kh, \ell h) - ikG_{M,1,n}^V(kh, \ell h)(1 - \delta_{n,M+1})), \\ I_m^{\mathcal{R}_1,H} &:= \sum_{k=0}^1 \sum_{\ell=0}^1 C_{k,\ell}^{\mathcal{R}_1,H} G_{M,m,0}^H(kh, \ell h), \quad J_{m,n}^{\mathcal{R}_1} := \sum_{k=0}^1 \sum_{\ell=0}^1 (C_{k,\ell}^{\mathcal{R}_1,V} Q_{M_f,m,n}^V(kh, \ell h) + C_{k,\ell}^{\mathcal{R}_1,H} Q_{M_f,m,n}^H(kh, \ell h)), \\ K_n^{\mathcal{R}_1,V} &:= - \sum_{k=0}^1 \sum_{\ell=0}^1 C_{k,\ell}^{\mathcal{R}_1,V} G_{M_{g_1},1,n}^V(kh, \ell h), \quad \text{and} \quad K_m^{\mathcal{R}_1,H} := - \sum_{k=0}^1 \sum_{\ell=0}^1 C_{k,\ell}^{\mathcal{R}_1,H} G_{M_{g_3},m,1}^H(kh, \ell h). \end{aligned}$$

By replacing the left-hand side of (4.11) with (4.13), replacing  $u^{(m,0)}$  for  $m = 2, \dots, M+1$  with (2.6), using (4.12), and rearranging some terms, we obtain

$$\begin{aligned} u^{(0,0)} &\left( I_0^{\mathcal{R}_1,V} + I_0^{\mathcal{R}_1,H} - ikI_1^{\mathcal{R}_1,H} + \sum_{p=1}^{\lfloor \frac{M+1}{2} \rfloor} (-1)^p k^{2p} I_{2p}^{\mathcal{R}_1,H} + i \sum_{p=1}^{\lfloor \frac{M}{2} \rfloor} (-1)^{p+1} k^{2p+1} I_{2p+1}^{\mathcal{R}_1,H} \right) + \sum_{\ell=0}^{\lfloor \frac{M}{2} \rfloor} u^{(0,2\ell+1)} I_{2\ell+1}^{\mathcal{R}_1,V} \\ &+ \sum_{\ell=1}^{\lfloor \frac{M}{2} \rfloor} u^{(0,2\ell)} \left( \sum_{p=\max\{\ell,1\}}^{\lfloor \frac{M+1}{2} \rfloor} (-1)^p \binom{p}{\ell} k^{2(p-\ell)} I_{2p}^{\mathcal{R}_1,H} + i \sum_{p=\max\{\ell,1\}}^{\lfloor \frac{M}{2} \rfloor} (-1)^{p+1} \binom{p}{\ell} k^{2(p-\ell)+1} I_{2p+1}^{\mathcal{R}_1,H} + I_{2\ell}^{\mathcal{R}_1,V} \right) \\ &+ u^{(0,2\lfloor \frac{M+1}{2} \rfloor)} \left( (-1)^{\lfloor \frac{M+1}{2} \rfloor} I_{2\lfloor \frac{M+1}{2} \rfloor}^{\mathcal{R}_1,H} + I_{2\lfloor \frac{M+1}{2} \rfloor}^{\mathcal{R}_1,V} \right) \left( 1 - \delta_{\lfloor \frac{M+1}{2} \rfloor, \lfloor \frac{M}{2} \rfloor} \right) + \sum_{\ell=0}^{\lfloor \frac{M_{g_1}-1}{2} \rfloor} g_1^{(2\ell+1)} (K_{2\ell+1}^{\mathcal{R}_1,V} - C_{g_1,2\ell+1}^{\mathcal{R}_1}) \\ &+ \sum_{\ell=0}^{\lfloor \frac{M_{g_1}}{2} \rfloor} g_1^{(2\ell)} \left( K_{2\ell}^{\mathcal{R}_1,V} + \sum_{p=\max\{\ell,1\}}^{\lfloor \frac{M_{g_1}}{2} \rfloor} (-1)^{p+1} \binom{p}{\ell} k^{2(p-\ell)} I_{2p+1}^{\mathcal{R}_1,H} - I_1^{\mathcal{R}_1,H} \delta_{\ell,0} - C_{g_1,2\ell}^{\mathcal{R}_1} \right) + \sum_{\ell=0}^{M_{g_3}} g_3^{(\ell)} (K_{\ell}^{\mathcal{R}_1,H} - C_{g_3,\ell}^{\mathcal{R}_1}) \\ &+ \sum_{j=0}^{\lfloor \frac{M_f-1}{2} \rfloor} \sum_{\ell=0}^{M_f-2j-2} f^{(\ell,2j+1)} (J_{\ell,2j+1}^{\mathcal{R}_1} - C_{f,\ell,2j+1}^{\mathcal{R}_1}) + \sum_{\gamma \in \{0,1\}} \sum_{\ell=0}^{\lfloor \frac{M_f+1-\gamma}{2} \rfloor - 1} \sum_{j=0}^{\lfloor \frac{M_f+1-\gamma}{2} \rfloor - \ell - 1} f^{(2\ell+\gamma,2j)} \left( \sum_{p=\max\{j+\ell+1,1\}}^{\lfloor \frac{M_f+1-\gamma}{2} \rfloor} \right. \\ &\left. (-1)^{p-\ell-1} \binom{p-\ell-1}{j} k^{2(p-\ell-j-1)} I_{2p+\gamma}^{\mathcal{R}_1,H} + J_{2\ell+\gamma,2j}^{\mathcal{R}_1} - C_{f,2\ell+\gamma,2j}^{\mathcal{R}_1} \right) = \mathcal{O}(h^{M+2}), \quad h \rightarrow 0. \end{aligned}$$

We set  $C_{k,\ell}^{\mathcal{R}_1,V} = \sum_{j=0}^{M+1} (a_{k,\ell,j} + ib_{k,\ell,j})(kh)^j$  and  $C_{k,\ell}^{\mathcal{R}_1,H} = \sum_{j=0}^{M+1} (c_{k,\ell,j} + id_{k,\ell,j})(kh)^j$ , where  $a_{k,\ell,j}, b_{k,\ell,j}, c_{k,\ell,j}, d_{k,\ell,j} \in \mathbb{R}$  for all  $k \in \{0, 1\}$  and  $\ell \in \{-1, 0, 1\}$ . By calculation,  $M = 5$  is the maximum positive integer such that the linear system, obtained by setting each coefficient of  $u^{(0,n)}$  for  $n = 0, \dots, 6$  to be  $\mathcal{O}(h^7)$  as  $h \rightarrow 0$ , has a non-trivial solution. Afterwards, to further simplify such a solution, we can set remaining coefficients associated with  $(kh)^5$  or  $(kh)^6$  to zero.

By using the minimization procedure described in the proofs of Theorems 2.2 and 2.3, we can verify that  $C_{0,1}^{\mathcal{R}_1,V} = C_{1,1}^{\mathcal{R}_1,V} = C_{0,0}^{\mathcal{R}_1,H} = C_{1,0}^{\mathcal{R}_1,H} = 0$ ,  $C_{0,0}^{\mathcal{R}_1,V} = C_{0,0}^{\mathcal{R}_1}$ ,  $C_{1,0}^{\mathcal{R}_1,V} = C_{1,0}^{\mathcal{R}_1}$ ,  $C_{0,1}^{\mathcal{R}_1,H} = C_{0,1}^{\mathcal{R}_1}$ , and  $C_{1,1}^{\mathcal{R}_1,H} = C_{1,1}^{\mathcal{R}_1}$ , where  $\{C_{k,\ell}^{\mathcal{R}_1}\}_{k,\ell \in \{0,1\}}$  are defined in (2.22). Given these  $\{C_{k,\ell}^{\mathcal{R}_1,V}\}_{k,\ell \in \{0,1\}}$  and  $\{C_{k,\ell}^{\mathcal{R}_1,H}\}_{k,\ell \in \{0,1\}}$ , we set  $M_f = M_{g_1} = M_{g_3} = 7$  and plug them into the following relations

$$\begin{aligned} C_{g_1,2\ell}^{\mathcal{R}_1} &= K_{2\ell}^{\mathcal{R}_1,V} + \sum_{p=\max\{\ell,1\}}^{\lfloor \frac{M_{g_1}}{2} \rfloor} (-1)^{p+1} \binom{p}{\ell} k^{2(p-\ell)} I_{2p+1}^{\mathcal{R}_1,H} - I_1^{\mathcal{R}_1,H} \delta_{\ell,0}, \quad \ell = 0, \dots, \lfloor \frac{M_{g_1}}{2} \rfloor, \\ C_{g_1,2\ell+1}^{\mathcal{R}_1} &= K_{2\ell+1}^{\mathcal{R}_1,V}, \quad \ell = 0, \dots, \lfloor \frac{M_{g_1}-1}{2} \rfloor, \quad C_{g_3,\ell}^{\mathcal{R}_1} = K_{\ell}^{\mathcal{R}_1,H}, \quad \ell = 0, \dots, M_{g_3}, \\ C_{f,\ell,2j+1}^{\mathcal{R}_1} &= J_{\ell,2j+1}^{\mathcal{R}_1}, \quad \ell = 0, \dots, M_f - 2j - 2, j = 0, \dots, \lfloor \frac{M_f}{2} - 1 \rfloor, \quad \text{and} \\ C_{f,2\ell+\gamma,2j}^{\mathcal{R}_1} &= \sum_{p=\max\{j+\ell+1,1\}}^{\lfloor \frac{M_f+1-\gamma}{2} \rfloor} (-1)^{p-\ell-1} \binom{p-\ell-1}{j} k^{2(p-\ell-j-1)} I_{2p+\gamma}^{\mathcal{R}_1,H} + J_{2\ell+\gamma,2j}^{\mathcal{R}_1}, \end{aligned} \tag{4.14}$$

where  $\gamma \in \{0, 1\}$ ,  $j = 0, \dots, \lfloor \frac{M_f+1-\gamma}{2} \rfloor - \ell - 1$ , and  $\ell = 0, \dots, \lfloor \frac{M_f+1-\gamma}{2} \rfloor - 1$ . This completes the proof of Theorem 2.4.  $\square$

*Proof of Theorem 2.5.* The proof is almost identical to the proof of Theorem 2.4. Note that we need to replace  $u^{(m,1)} = -g_3^{(m)}$  with  $u^{(m,1)} = ik u^{(m,0)} + g_4^{(m)}$  for all  $m \in \mathbb{N}_0$  in (4.12).  $\square$

## REFERENCES

- [1] M. Ainsworth, Discrete dispersion relation for  $hp$ -version finite element approximation at high wave number. *SIAM J. Numer. Anal.* **42** (2004), no. 2, 553-575.
- [2] I. M. Babuška and S. A. Sauter, Is the pollution effect of the FEM avoidable for the Helmholtz equation considering high wave numbers? *SIAM Rev.* **42** (2000), no. 3, 451-484.
- [3] S. Britt, S. Tsynkov, and E. Turkel, A compact fourth order scheme for the Helmholtz equation in polar coordinates. *J. Sci. Comput.* **45** (2010), 26-47.
- [4] S. Britt, S. Tsynkov, and E. Turkel, Numerical simulation of time-harmonic waves in inhomogeneous media using compact high order schemes. *Commun. Comput. Phys.* **9** (2011), no. 3, 520-541.
- [5] S. Britt, S. Tsynkov, and E. Turkel, A high order numerical method for the Helmholtz equation with nonstandard boundary conditions. *SIAM J. Sci. Comput.* **35** (2013), no. 5, A2255-A2292.
- [6] Z. Chen, D. Cheng, W. Feng, and T. Wu, An optimal 9-point finite difference scheme for the Helmholtz equation with PML. *Int. J. Numer. Anal. Mod.* **10** (2013), no. 2, 389-410.
- [7] Z. Chen, T. Wu, and H. Yang, An optimal 25-point finite difference scheme for the Helmholtz equation with PML. *J. Comput. Appl. Math.* **236** (2011), 1240-1258.
- [8] P.-H. Cocquet, M. J. Gander, and X. Xiang, Closed form dispersion corrections including a real shifted wavenumber for finite difference discretizations of 2D constant coefficient Helmholtz problems. *SIAM J. Sci. Comput.* **43** (2021), no. 1, A278-A308.
- [9] H. Dastour and W. Liao, A fourth-order optimal finite difference scheme for the Helmholtz equation with PML. *Comput. Math. Appl.* **78** (2019), no. 6, 2147-2165.
- [10] H. Dastour and W. Liao, An optimal 13-point finite difference scheme for a 2D Helmholtz equation with a perfectly matched layer boundary condition. *Numer. Algorithms* **86** (2021), 1109-1141.
- [11] Y. Du and H. Wu, Preasymptotic error analysis of higher order FEM and CIP-FEM for Helmholtz equation with high wave number. *SIAM J. Numer. Anal.* **53** (2015), no. 2, 782-804.
- [12] V. Dwarka and C. Vuik, Pollution and accuracy of solutions of the Helmholtz equation: a novel perspective from the eigenvalues. *J. Comput. Appl. Math.* **395** (2021), 1-21.

- [13] O. G. Ernst and M. J. Gander, Why is it difficult to solve Helmholtz problems with classical iterative methods. Numerical analysis of multiscale problems, *Lecture Notes in Computational Science and Engineering* **83**, Springer, Berlin, Heidelberg, 2011, 325-363.
- [14] Q. Feng, B. Han, and P. Mineev, Sixth order compact finite difference schemes for Poisson interface problems with singular sources. *Comp. Math. Appl.* **99** (2021), 2-25.
- [15] Q. Feng, B. Han, and P. Mineev, A high order compact finite difference scheme for elliptic interface problems with discontinuous and high-contrast coefficients, arXiv:2105.04600 (2021), 30 pp.
- [16] X. Feng and H. Wu, Discontinuous Galerkin methods for the Helmholtz equation with large wave number. *SIAM J. Numer. Anal.* **47** (2009), no. 4, 2872-2896.
- [17] X. Feng and H. Wu, *hp*-discontinuous Galerkin methods for the Helmholtz equation with large wave number. *Math. Comp.* **80** (2011), no. 276, 1997-2024.
- [18] M. J. Gander and H. Zhang, A class of iterative solvers for the Helmholtz equation: factorizations, sweeping preconditioners, source transfer, single layer potentials, polarized traces, and optimized Schwarz methods. *SIAM Rev.* **61** (2019), no. 1, 3-76.
- [19] I. G. Graham and S. A. Sauter, Stability and finite element error analysis for the Helmholtz equation with variable coefficients. *Math. Comp.* **89** (2020), no. 321, 105-138.
- [20] B. Han, M. Michelle, and Y. S. Wong, Dirac assisted tree method for 1D heterogeneous Helmholtz equations with arbitrary variable wave numbers. *Comput. Math. Appl.* **97** (2021), 416-438.
- [21] B. Han and M. Michelle, Sharp wavenumber-explicit stability bounds for 2D Helmholtz equations, arXiv:2108.06469 (2021), 19 pp.
- [22] U. Hetmaniuk, Stability estimates for a class of Helmholtz problems. *Commun. Math. Sci.* **5** (2007), no. 3, 665-678.
- [23] R. Hiptmair, A. Moiola, and I. Perugia, A survey of Trefftz methods for the Helmholtz equation. Building bridges: connections and challenges in modern approaches to numerical partial differential equations, *Lecture Notes in Computational Science and Engineering* **114**, Springer, Cham, 2016, 237-279.
- [24] F. Ihlenburg and I. M. Babuška, Finite element solution of the Helmholtz equation with high wave number part II: the *hp* version of the FEM. *SIAM J. Numer. Anal.* **34** (2006), no. 1, 315-358.
- [25] Z. Li and K. Pan, Can 4th-order compact schemes exist for flux type BCs, arXiv:2109.05638 (2021), 22 pp.
- [26] M. Medvinsky, S. Tsynkov, and E. Turkel, The method of difference potentials for the Helmholtz equation using compact high order schemes. *J.Sci. Comput.* **53** (2012), 150-193.
- [27] J. M. Melenk and S. Sauter, Wavenumber explicit convergence analysis for Galerkin discretizations of the Helmholtz equation. *SIAM J. Numer. Anal.* **49** (2011), no. 3, 1210-1243.
- [28] A. Moiola and E. A. Spence, Acoustic transmission problems: wavenumber-explicit bounds and resonance-free regions. *Math. Models Methods Appl. Sci.* **29** (2019), no. 2, 317-354.
- [29] K. Pan, D. He, and Z. Li, A high order compact FD framework for elliptic BVPs involving singular sources, interfaces, and irregular domains. *J. Sci. Comput.* **88** (2021), no. 67, 1-25.
- [30] D. Peterseim, Eliminating the pollution effect in Helmholtz problems by local subscale correction. *Math. Comp.* **86** (2017), no. 305, 1005-1036.
- [31] C. C. Stolk, M. Ahmed, and S. K. Bhowmik, A multigrid method for the Helmholtz equation with optimized coarse grid corrections. *SIAM J. Sci. Comput.* **36** (2014), no. 6, A2819-A2841.
- [32] E. Turkel, D. Gordon, R. Gordon, and S. Tsynkov, Compact 2D and 3D sixth order schemes for the Helmholtz equation with variable wave number. *J. Comp. Phys.* **232** (2013), no. 1, 272-287.
- [33] K. Wang and Y. S. Wong, Pollution-free finite difference schemes for non-homogeneous Helmholtz equation. *Int. J. Numer. Anal. Mod.* **11** (2014), no. 4, 787-815.
- [34] K. Wang and Y. S. Wong, Is pollution effect of finite difference schemes avoidable for multi-dimensional Helmholtz equations with high wave numbers? *Commun. Comput. Phys.* **21** (2017), no. 2, 490-514.
- [35] T. Wu and R. Xu, An optimal compact sixth-order finite difference scheme for the Helmholtz equation. *Comput. Math. Appl.* **75** (2018), no. 7, 2520-2537.
- [36] Y. Zhang, K. Wang, and R. Guo, Sixth-order finite difference scheme for the Helmholtz equation with inhomogeneous Robin boundary condition. *Adv. Differ. Equ.* **362** (2019), 1-15.

DEPARTMENT OF MATHEMATICAL AND STATISTICAL SCIENCES, UNIVERSITY OF ALBERTA, EDMONTON, ALBERTA, CANADA T6G 2G1. [qfeng@ualberta.ca](mailto:qfeng@ualberta.ca) [bhan@ualberta.ca](mailto:bhan@ualberta.ca) [mmichell@ualberta.ca](mailto:mmichell@ualberta.ca)